

1 **MORPHOMETRIC AND MORPHOLOGICAL-BASED**
2 **NON-INVASIVE SEX IDENTIFICATION OF BLOOD**
3 **COCKLES *TEGILLARCA GRANOSA* (LINNAEUS,**
4 **1758)**

5 A Special Problem Proposal
6 Presented to
7 the Faculty of the Division of Physical Sciences and Mathematics
8 College of Arts and Sciences
9 University of the Philippines Visayas
10 Miag-ao, Iloilo

11 In Partial Fulfillment
12 of the Requirements for the Degree of
13 Bachelor of Science in Computer Science by

14 ADRICULA, Briana Jade
15 PAJARILLA, Gliezel Ann
16 VITO, Ma. Christina Kane

17 Francis DIMZON, Ph.D.
18 Adviser
19 Victor Marco Emmanuel FERRIOLS, Ph.D.
20 Co-Adviser

Abstract

23 *Tegillarca granosa*, commonly known as blood cockles, is a significant marine
24 bivalve species due to its nutritional benefits and economic importance. Accurate
25 sex determination is essential for maintaining a balanced male-to-female ratio,
26 sustainable harvesting, and resource management. However, the sex-determining
27 mechanisms based on shell morphology are challenging macroscopically, and no
28 existing technologies are available for non-invasive sex classification. This study
29 proposes the use of machine learning and deep learning techniques to classify the
30 sex of blood cockles based on various shell measurements (length, width, height,
31 hinge line distance, umbo distance, and rib count) and images from multiple
32 camera angles (dorsal, ventral, anterior, posterior, and lateral views). The initial
33 machine learning analysis using K-Nearest Neighbor (KNN) achieved an accuracy
34 of 64.16%, a precision of 64.97%, a recall of 64.16%, and an F1-score of 63.75%.
35 In contrast, deep learning with Convolutional Neural Networks (CNN) achieved
36 an accuracy of 71.68%, a precision of 72.52%, a recall of 69.29%, an F1-score of
37 69.12%, and an AUC score of 77.34% using images captured from the left lateral
38 angle. These results offer a non-invasive method for sex identification, which could
39 help in sustainable resource management and serve as a baseline for future studies
40 on blood cockles classification.

Keywords: deep learning, supervised machine learning, computer vision,
convolutional neural network, blood cockle, sex identification, *Tegillarca granosa*

⁴² Contents

⁴³ 1 Introduction	1
⁴⁴ 1.1 Overview	1
⁴⁵ 1.2 Problem Statement	2
⁴⁶ 1.3 Research Objectives	3
⁴⁷ 1.3.1 General Objective	3
⁴⁸ 1.3.2 Specific Objectives	3
⁴⁹ 1.4 Scope and Limitations of the Research	3
⁵⁰ 1.5 Significance of the Research	4
⁵¹ 2 Review of Related Literature	6
⁵² 2.1 Background on <i>Tegillarca granosa</i> and Their Importance	7
⁵³ 2.2 Current Methods of Sex Identification in <i>Tegillarca granosa</i>	9
⁵⁴ 2.3 Machine Learning and Deep Learning in Biological Studies	11
⁵⁵ 2.3.1 Deep Learning for Phenotype Classification in Ark Shells .	12
⁵⁶ 2.3.2 Geometric Morphometrics and Machine Learning for Species ⁵⁷ Delimitation	12
⁵⁸ 2.3.3 Contour Analysis in Mollusc Shells Using Machine Learning	12
⁵⁹ 2.3.4 Machine Learning for Shape Analysis of Marine Organisms	13

60	2.3.5 Deep Learning for Landmark-Free Morphological Feature Extraction	14
62	2.3.6 Machine Learning for Sex Differentiation in Abalone	15
63	2.3.7 Machine Learning for Geographical Traceability in Bivalves	16
64	2.4 Limitations on Sex Identification in <i>Tegillarca granosa</i>	16
65	2.5 Chapter Summary	18
66	3 Research Methodology	21
67	3.1 Sample Collection	21
68	3.2 Ethical Considerations	23
69	3.3 Creating <i>T. granosa</i> Dataset	23
70	3.4 Morphometric and Morphological Characteristics Collection	24
71	3.5 Image Acquisition and Data Gathering	25
72	3.6 Hardware and Software Configuration	26
73	3.7 Morphometric Characteristics Evaluation Using Machine Learning	26
74	3.7.1 Data Preprocessing	27
75	3.7.2 Machine Learning Models Training	28
76	3.8 Morphological Characteristics Evaluation Using Deep Learning	29
77	3.8.1 Convolutional Neural Network	30
78	3.8.2 CNN Training	32
79	3.9 Evaluation Metrics	34
80	4 Results and Discussions	36
81	4.1 Machine Learning Analysis	36
82	4.1.1 Data Exploration	36

83	4.1.2 Statistical Analysis	37
84	4.1.3 Feature Importance Analysis	38
85	4.1.4 Performance Evaluation	39
86	4.1.5 Confusion Matrix Analysis	40
87	4.2 Deep Learning Analysis	41
88	4.2.1 Baseline Model	41
89	4.2.2 Comparison of Individual and Combined Angles	42
90	4.2.3 Training Result and Hyperparameter Tuning	42
91	4.2.4 Proposed Model	44
92	4.2.5 Learning Rates and Training Behavior per Fold	44
93	4.2.6 Visualizations	45
94	4.3 Discussions	48
95	5 Conclusion and Recommendations	50
96	5.1 Conclusion	50
97	5.2 Recommendations	51
98	References	53
99	A Data Gathering Documentation	58
100	B Supplementary Analysis	61

¹⁰¹ List of Figures

¹⁰²	2.1 Diagram of <i>Tegillarca granosa</i> 's External Anatomy	7
¹⁰³	3.1 Male and Female <i>Tegillarca granosa</i> shells	22
¹⁰⁴	3.2 Different Views of the <i>T. granosa</i> Shell Captured	24
¹⁰⁵	3.3 Linear Measurements of <i>Tegillarca granosa</i> shell.	25
¹⁰⁶	3.4 Image Acquisition Setup for <i>T. granosa</i> Samples	26
¹⁰⁷	3.5 Data Preprocessing Pipeline	27
¹⁰⁸	3.6 Diagram of k-fold cross-validation with k = 5	29
¹⁰⁹	3.7 Shadows removed from male samples at different angles	30
¹¹⁰	3.8 Shadows removed from female samples at different angles	30
¹¹¹	3.9 Architecture of Convolutional Neural Network (CNN)	31
¹¹²	3.10 Diagram of stratified k-fold cross-validation with k=5	32
¹¹³	3.11 Data Augmentation Techniques	33
¹¹⁴	4.1 Correlation heatmap of morphometric features with the sex of <i>T. granosa</i>	37
¹¹⁶	4.2 Feature Importance Scores Using the Kruskal-Wallis Test	38
¹¹⁷	4.3 Feature Importance Scores Using the Kruskal-Wallis Test	40
¹¹⁸	4.4 Training and Validation Accuracy per Fold	45

119	4.5 Average Training and Validation Accuracy Across Folds	46
120	4.6 Training and Validation Loss per Fold	46
121	4.7 Average Training and Validation Loss Across Folds	47
122	4.8 Confusion Matrix for Final Model Predictions	47
123	4.9 ROC Curve and AUC Score	48
124	A.1 Sex Identification Through Spawning of <i>Tegillarca granosa</i>	58
125	A.2 Sex-Based Separation of <i>Tegillarca granosa</i> Samples Post-Spawning	58
126	A.3 Sex Identified Female Through Dissection of <i>Tegillarca granosa</i> .	59
127	A.4 Sex Identified Male Through Dissection of <i>Tegillarca granosa</i> .	59
128	A.5 Linear Measurements of Female <i>Tegillarca granosa</i>	59
129	A.6 Linear Measurements of Male <i>Tegillarca granosa</i>	60
130	A.7 Captured Images of Female <i>Tegillarca granosa</i>	60
131	A.8 Captured Images of Male <i>Tegillarca granosa</i>	60
132	B.1 Feature Distribution of <i>Tegillarca granosa</i>	61
133	B.2 Correlation Matrix of Morphological Variables <i>Tegillarca granosa</i>	62
134	B.3 Feature Maps from First Convolution Layer	62
135	B.4 Feature Maps from Second Convolution Layer	63
136	B.5 Feature Maps from Third Convolution Layer	63

¹³⁷ List of Tables

¹³⁸	2.1 Comparison of the Methods Used in Bivalves Studies	19
¹³⁹	4.1 Mann-Whitney U Test Results for Sex-Based Feature Comparison	38
¹⁴⁰	4.2 Performance Metrics for Models with All 13 Features	39
¹⁴¹	4.3 Performance Metrics for Models with 5 Features	39
¹⁴²	4.4 Performance Metrics for Unbalanced vs. Balanced Datasets (Batch Size: 16, Epochs: 20)	41
¹⁴⁴	4.5 Performance Metrics for Individual and Combined Angles (Batch Size: 16, Epochs: 20)	42
¹⁴⁶	4.6 Effect of Batch Size and Epoch Values on CNN Model Performance	43
¹⁴⁷	4.7 Performance Metrics for Different Activation Functions (Batch Size: 32, Epochs: 50)	43
¹⁴⁹	4.8 Per-Fold Performance Metrics (Batch Size: 32, Epochs: 50, Activation Function: ReLU)	44
¹⁵¹	4.9 Learning Rate Reductions, Early Stopping, and Best Epochs per Fold During 5-Fold Cross-Validation	45
¹⁵²		

¹⁵³ **Chapter 1**

¹⁵⁴ **Introduction**

¹⁵⁵ **1.1 Overview**

¹⁵⁶ The Philippines is a global center of marine biodiversity and has established aqua-
¹⁵⁷ culture as a significant contributor to total fishery production (Aypa & Baconguis,
¹⁵⁸ 2000; BFAR, 2019). The country produces over 4 million tonnes of seafood annu-
¹⁵⁹ ally and is the 11th largest seafood producer in the world. Aquaculture is deeply
¹⁶⁰ integrated into Filipinos' livelihoods, encompassing fish cultivation and the pro-
¹⁶¹ duction of various aquatic species, including bivalves. Among these, blood cockles
¹⁶² (*Tegillarca granosa*) hold considerable economic and environmental significance,
¹⁶³ making it essential to ensure sustainable production and population balance.

¹⁶⁴ Maintaining a balanced male-to-female ratio of blood cockles is crucial to pre-
¹⁶⁵ vent overharvesting and ensure sustainability. An imbalanced ratio can lead to
¹⁶⁶ overexploitation and negatively impact the population's viability. However, there
¹⁶⁷ is limited literature on *T. granosa* that provides a thorough understanding of its
¹⁶⁸ sex-determining mechanisms, particularly regarding sexual dimorphism based on
¹⁶⁹ morphometric and morphological characteristics (Breton, Capt, Guerra, & Stew-
¹⁷⁰ art, 2017).

¹⁷¹ Currently, sex determination methods for blood cockles are invasive, including
¹⁷² dissection and histological examinations, which often result in the death of the
¹⁷³ species. While there is growing literature on sex identification in aquaculture
¹⁷⁴ commodities using machine learning and deep learning, there is a notable scarcity
¹⁷⁵ of research specific to *T. granosa* (Miranda & Ferriols, 2023).

¹⁷⁶ This study aims to provide a detailed baseline analysis of blood cockles by

¹⁷⁷ leveraging their morphometric and morphological characteristics. Sexual dimor-
¹⁷⁸ phism in bivalves is often subtle and challenging to establish macroscopically (Karapunar,
¹⁷⁹ Werner, Fürsich, & Nützel, 2021). However, by integrating machine learning and
¹⁸⁰ deep learning, the study seeks to identify distinct features that may indicate sexual
¹⁸¹ dimorphism between male and female blood cockles.

¹⁸² 1.2 Problem Statement

¹⁸³ Identifying the sex of *T. granosa* is important for promoting sustainable aquacul-
¹⁸⁴ ture and biodiversity by maintaining a balanced male-to-female ratio. A balanced
¹⁸⁵ ratio helps prevent overharvesting. Although sex identification is crucial for blood
¹⁸⁶ cockle population management and sustainable aquaculture, there is a notable
¹⁸⁷ lack of research on creating non-invasive methods for determining the sex of *T.*
¹⁸⁸ *granosa*. Many recent studies and approaches rely on invasive methods like dis-
¹⁸⁹ section or histological analysis, which are impractical for large-scale aquaculture
¹⁹⁰ operations focused on conservation.

¹⁹¹ Current methods for determining the sex of *T. granosa* are invasive and in-
¹⁹² volve dissection, which requires cutting open the shell to visually inspect the
¹⁹³ gonads (Erica, 2018). This procedure can cause harm to the specimens and fre-
¹⁹⁴ quently leads to their death. Another method is histological examination, where
¹⁹⁵ tissue samples are analyzed under a microscope (May, Maung, Phy, & Tun,
¹⁹⁶ 2021). Both approaches are labor-intensive and time-consuming, and can pose
¹⁹⁷ risks to population management, particularly when maintaining a balanced sex
¹⁹⁸ ratio for breeding programs is essential. Moreover, these invasive methods require
¹⁹⁹ specialized technical skills for accurate execution. Resource-limited aquaculture
²⁰⁰ operations face significant challenges in accessing the necessary laboratory equip-
²⁰¹ ment, such as microscopes and staining tools, complicating the process.

²⁰² A less invasive approach employed by aquaculturists involves monitor spawning
²⁰³ behavior, where individuals are separated and stimulated to reproduce in order
²⁰⁴ to determine their sex through the release of gametes (Miranda & Ferriols, 2023).
²⁰⁵ Although this method is indeed less invasive than dissection, it still induces stress
²⁰⁶ in blood cockles and may not be completely effective for fast identification in large
²⁰⁷ populations.

²⁰⁸ Given the limitations of both invasive and less invasive methods, there is a
²⁰⁹ clear need for a more advanced approach. An alternative, non-invasive method
²¹⁰ involving machine and deep learning technologies could address these issues by
²¹¹ providing a fast, accurate, and effective solution without harming or stressing the

²¹² blood cockles.

²¹³ 1.3 Research Objectives

²¹⁴ 1.3.1 General Objective

²¹⁵ The general objective of this study is to develop a non-invasive method for iden-
²¹⁶ tifying the sex of *Tegillarca granosa* using machine and deep learning integrated
²¹⁷ with computer vision technologies. This method aims to provide accurate and
²¹⁸ streamlined sex identification without causing harm to the specimens, thus sup-
²¹⁹ porting sustainable aquaculture practices.

²²⁰ 1.3.2 Specific Objectives

²²¹ To achieve the overall general objective of developing a non-invasive sex identifi-
²²² cation of *T. granosa* using machine learning, deep learning, and computer vision
²²³ technologies, the following specific objectives have been established:

- ²²⁴ 1. to collect and organize a comprehensive dataset of *T. granosa*, which will
²²⁵ include linear measurements and images captured from different camera an-
²²⁶ gles that will serve as the basis for training and evaluating the machine
²²⁷ learning and deep learning models.
- ²²⁸ 2. to develop and implement machine learning and deep learning models that
²²⁹ can classify the sex of *T. granosa* based on the collected linear measurements
²³⁰ and images of different camera angles of the sample, and determine the best
²³¹ performing models.
- ²³² 3. to evaluate the model performance using performance metrics such as accu-
²³³ racy, precision, recall, and F1-score, AUC-ROC score for deep learning, and
²³⁴ optimize the performance by performing hyperparameter optimization.

²³⁵ 1.4 Scope and Limitations of the Research

²³⁶ This study is conducted alongside the ongoing research by the UPV DOST-
²³⁷ PCAARRD, titled "Establishment of the Center for Mollusc Research and De-

238 development: Development of Spawning and Hatchery Techniques for the Blood
239 Cockle (*Anadara granosa*) for Sustainable Aquaculture." The ongoing research pri-
240 marily involves the rearing of *T. granosa* from spat to larvae, feeding experiments,
241 stocking density evaluations, substrate selection, and settlement rate assessments.

242 In contrast, this study mainly focused on developing a non-invasive method for
243 identifying the sex of *Tegillarca granosa* using machine learning, computer vision,
244 and deep learning technologies. The goal is to provide an accurate and efficient
245 means of sex identification without causing harm to the samples, contributing to
246 sustainable aquaculture practices.

247 The researchers worked with 271 blood cockles that had been sex-identified
248 and taken from Panay Island, specifically sourced from Zarraga Iloilo and Ivisan
249 Capiz. These samples, divided between 144 males and 127 females, were obtained
250 through induced spawning via temperature shock and dissection. Data collection
251 was limited to the spawned stage among the five gonadal stages - immature, devel-
252 oping, mature, spawning, and spent stages. The other stages were not preferable
253 due to indistinguishable gonads and their inability to undergo induced spawning
254 (May et al., 2021). Thus, the researchers only focused on the samples undergoing
255 the spawned stage.

256 During the data collection, the researchers personally gathered linear measure-
257 ments, including length, width, height, rib count, length of the hinge line, and dis-
258 tance between the umbos through the vernier caliper. The data-gathering process
259 was supervised by the University Research Associates from the Institute of Aquas-
260 culture, College of Fisheries and Ocean Sciences. Aside from linear measurements,
261 images were taken from six different angles. The process of linear measurements
262 and image collection were non-invasive, considering the blood cockle-built ability
263 to survive in low oxygen environments and naturally inhabit intertidal mudflats
264 (Zhan & Bao, 2022).

265 The method developed in this study is specific to *Tegillarca granosa* and may
266 not apply to other bivalve species. The model was trained exclusively for *Te-*
267 *gillarca granosa* and morphometric and morphological features, which may not be
268 consistent and applicable across other shellfish species.

269 1.5 Significance of the Research

270 This study will give us a significant advancement in non-invasive sex identifica-
271 tion methods in *T. granosa* providing innovative solutions that could solve the
272 challenges in identifying sex and reshape sustainable approaches to aquaculture.

²⁷³ The significance of this study extends to the following:

²⁷⁴ *Research Institution.* The result of this study focusing on the sex-identification
²⁷⁵ mechanism of bivalves, specifically *Tegillarca granosa*, will provide valuable in-
²⁷⁶ sights into universities and research centers that focus on fisheries and coastal
²⁷⁷ management, such as the UPV Institute of Aquaculture, that aim to develop
²⁷⁸ sustainable development and suitable culture techniques.

²⁷⁹ *Fishermen.* By developing a non-invasive method in sex identification, this
²⁸⁰ study can help long-term harvest efficiency and maintain the ratio of the harvest
²⁸¹ which can help prevent exploitation of the *T. granosa*.

²⁸² *Coastal Communities.* The result of this study would be beneficial for the
²⁸³ coastal communities that are reliant on their source of income with aquaculture
²⁸⁴ commodities like blood cockles. Maintaining the diversity and aspect ratio of
²⁸⁵ male and female may increase the market value of blood cockle production since
²⁸⁶ cockle aquaculture faces significant obstacles worldwide due to the fluctuating
²⁸⁷ seed supplies and scarcity of broodstock from the wild.

²⁸⁸ *Future Researchers.* The result of this study would serve as the basis for studies
²⁸⁹ that involve sex identification in bivalves such as *T. granosa*. Some technologies
²⁹⁰ are yet to be explored in machine learning, deep learning, and computer vision
²⁹¹ technologies that can lead to higher accuracy and distinguish the presence of
²⁹² sexual dimorphism in the *T. granosa*.

²⁹³ **Chapter 2**

²⁹⁴ **Review of Related Literature**

²⁹⁵ Aquaculture is the fastest-growing industry in animal food production and has
²⁹⁶ great potential as a sustainable solution to global food security, nutrition, and
²⁹⁷ development (*FAO 2024 Report: Sustainable Aquatic Food Systems Important*
²⁹⁸ *for Global Food Security – European Fishmeal*, 2024). Aquaculture is deeply in-
²⁹⁹ tegrated into the livelihoods of Filipinos, not only through fish cultivation but
³⁰⁰ also through the production of other aquatic species, including mollusks, oysters,
³⁰¹ clams, scallops, and mussels (Breton et al., 2017). Mollusks, particularly blood
³⁰² clams *Tegillarca granosa*, have economic and environmental significance. It has
³⁰³ been a collective effort to maintain an ideal male-to-female ratio to avoid overhar-
³⁰⁴ vesting and maintain the optimal ratio to preserve the population and production
³⁰⁵ of the blood cockles.

³⁰⁶ The members of the Arcidae Family, including *T. granosa* are important
³⁰⁷ sources of food and livelihood. Cockle aquaculture meets rising demands, however,
³⁰⁸ it faces significant challenges due to fluctuating seed supplies (Miranda & Ferriols,
³⁰⁹ 2023). To solve the problem, researchers exert a considerable amount of effort,
³¹⁰ developing a broader understanding of bivalves, including their sex-determining
³¹¹ mechanism, due to their notable importance in terms of diversity, environmental
³¹² benefits, and economic and market importance (Breton et al., 2017). Despite the
³¹³ promising idea of identifying sex, there is limited research reported in terms of
³¹⁴ sexual dimorphism, making it harder to distinguish through its morphological and
³¹⁵ morphometric characteristics.

³¹⁶ By addressing the challenges in the sex identification of *T. granosa*, it would be
³¹⁷ able to address one problem at a time. Currently, there are no recent documented
³¹⁸ publications that integrate machine learning and computer vision in characterizing
³¹⁹ sexual dimorphism, reducing complexity, variability in sex determination, and

³²⁰ differentiation mechanisms in bivalves, including *T. granosa* specifically.

³²¹ **2.1 Background on *Tegillarca granosa* and Their 322 Importance**

³²³ *Tegillarca granosa* (Linnaeus, 1758) is also known as blood cockles or blood clam.
³²⁴ In the Philippines, it is known locally as Litob and Bakalan, a marine bivalve
³²⁵ species from the family Arcidae. Litob is widely distributed in the world including
³²⁶ Southeast Asia. They can be found in the intertidal mudflats adjacent to the
³²⁷ mangrove forest (Srisunont, Nobpakhun, Yamalee, & Srisunont, 2020). With
³²⁸ the intertidal mudflat as T.granosa's habitat, they experience severe hypoxia or
³²⁹ low oxygen levels in the blood tissues during the tidal cycle. The blood clams
³³⁰ exhibit a unique red-blood phenotype where it serves two purposes the hemocyte
³³¹ carries oxygen around the body and strengthens immune defenses. In addition,
³³² it possesses a unique ability to absorb oxygen at similar rates in water and air
³³³ (Zhan & Bao, 2022).

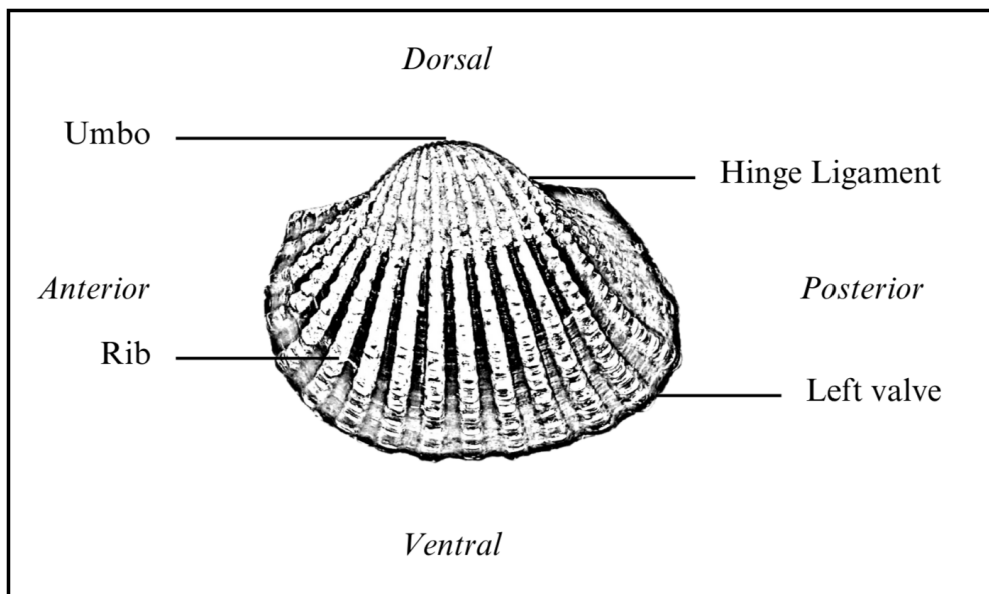


Figure 2.1: Diagram of *Tegillarca granosa*'s External Anatomy

³³⁴ *T. granosa* shell is medium-sized, fairly thick, ovate, and convex, with both
³³⁵ valves being equal in size but asymmetrical from the hinge. The top edge of
³³⁶ the dorsal margin is straight, while the front is rounded and slopes downward,
³³⁷ with its back being obliquely rounded with a concave bottom edge. It has a
³³⁸ narrow diamond-shaped ligament near the hinge with 3-4 dark chevron markings,

339 although some may be incomplete. The shell's outer layer, or the periostracum, is
340 smooth and brown with a straight hinge line and 40–68 fine short teeth arranged
341 in a straight line. The beak, or prosogyrate, curves forward, with the shell having
342 18–21 raised ribs with blunt nodules and spaces between them. The inner shell is
343 white with crenulations along the valves' ventral, anterior, and posterior margins.
344 The posterior adductor scar is elongated and squarish, while the anterior adductor
345 scar is similar but smaller in size. The mantle covering the bulk of *T. granosa*'s
346 visceral mass is thin but the edges are thick and muscular. It bears the impression
347 of the crenulated shell edges. Their foot is large with a ventral groove with no byssus
348 or thread-like attachment. The *T. granosa*'s soft body is blood red (Narasimham,
349 1988).

350 *T. granosa* is one of the most well-known marine bivalves given that they are
351 a protein-rich food, known for their rich flavor, substantial nutritional benefits, a
352 good source of vitamins, low in fat, and contain a considerable amount of iron,
353 important in combating anemia (Zha et al., 2022). Blood cockles were collected
354 by locals inhabiting the brackish mudflats during the low tides for consumption
355 and sold in the market as a source of livelihood (Miranda & Ferriols, 2023). *T.*
356 *granosa* is not only valuable for its market and food purposes but also facilitates
357 an important role in marine ecosystems as a food source for various organisms
358 like wading birds, intertidal-feeding fish, and crustaceans such as shore crabs and
359 shrimp (Burdon, Callaway, Elliott, Smith, & Wither, 2014). Blood cockles can act
360 as sentinel species and a bioindicator of marine pollutants such as heavy metals
361 (Ishak, Mohamad, Soo, & Hamid, 2016) and polycyclic aromatic hydrocarbons
362 (PAHs) (Sany et al., 2014). Additionally, cockle shells can be utilized to create a
363 cost-effective catalyst for biodiesel production by providing calcium oxide (Boey,
364 Maniam, Hamid, & Ali, 2011).

365 Determining the sex of bivalves is important for three reasons: diversity, en-
366 vironmental benefits, and economic significance (Breton et al., 2010). Firstly,
367 with the estimated 25, 000 living species under class Bivalvia, it would be a suit-
368 able resource to develop a broader understanding of their evolution of the sex
369 and sex determination mechanism (Breton et al., 2010). Second, studying sex
370 determination is important since bivalves are utilized as bioindicators of environ-
371 mental health. This would pave the way for understanding bivalves' life cycle and
372 population dynamics in determining different factors that affect them (Campos,
373 Tedesco, Vasconcelos, & Cristobal, 2012). Thirdly, the immediate and practical
374 reason to unveil the sex determination mechanism is the economic and nutritional
375 importance of bivalves as a large population of people relies on fish and shellfish
376 as sources of food and nutrition (Naylor et al., 2000). Additionally, male and
377 female aquaculture commodities have different growth and economic values. Male
378 Nile tilapia, for example, grow faster and have lower feed conversion rates than

³⁷⁹ females, female Kuruma prawns (*Penaeus japonicus*) are generally larger than
³⁸⁰ males at the time of harvest (Budd, Banh, Domingos, & Jerry, 2015).

³⁸¹ Clearly, much more work is required to understand the mechanisms under-
³⁸² lying sexual dimorphism in bivalves, specifically *T. granosa*. Just like the other
³⁸³ aquaculture commodities, sex affects not just reproduction but it can affect mar-
³⁸⁴ ket preference and underlying economic value, making the determination of sex
³⁸⁵ important for meeting consumer demands. These are the increasing significance
³⁸⁶ of the *T. granosa* despite the lack of reviewed articles in the Philippines.

³⁸⁷ **2.2 Current Methods of Sex Identification in *Tegillarca granosa*** ³⁸⁸

³⁸⁹ The current sex identification methods in *Tegillarca granosa* range from invasive
³⁹⁰ histological techniques to less invasive methodologies like temperature-induced
³⁹¹ spawning. Each approach comes with its pros and cons regarding accuracy, feasi-
³⁹² bility, and impact on natural populations.

³⁹³ Induced spawning and larval rearing are considered the less invasive techniques
³⁹⁴ used to study *Tegillarca granosa*. In the Philippines, limited research has been
³⁹⁵ done on the *Tegillarca granosa* (Linnaeus, 1758), and this study, titled Initial
³⁹⁶ Attempts on Spawning and Larval Rearing of the Blood Cockle, *Tegillarca granosa*
³⁹⁷ in the Philippines, is conducted by Miranda and Ferriols (2023). The researchers
³⁹⁸ conducted experiments on induced spawning and larval rearing, discovering that
³⁹⁹ the eggs of female *T. granosa* were salmon pink, while the sperm released by males
⁴⁰⁰ looked milky. After spawning, the researchers successfully generated 6, 531, 000
⁴⁰¹ fertilized eggs.

⁴⁰² The researchers highlighted the importance of *T. granosa* and other anadarinids
⁴⁰³ as a food source that was established worldwide, especially in Malaysia and Korea.
⁴⁰⁴ However, in the Philippines, the bivalve aquaculture of the clam species is still
⁴⁰⁵ limited. The experiment which focuses on the culture and rearing of *T. granosa*
⁴⁰⁶ was attempted by subjecting the wild broodstocks to a series of temperature fluc-
⁴⁰⁷ tuations to induce the spawning of gametes. This is currently the most natural
⁴⁰⁸ and least invasive method for bivalves (Aji, 2011). The study of Miranda and
⁴⁰⁹ Ferriols aimed to pave the way to the sustainable production of *T. granosa* seeds
⁴¹⁰ for aquaculture production and stock enhancement despite the scarcity of docu-
⁴¹¹ mented hatchery culture of *T. granosa* from larvae to adults that is available in
⁴¹² the Philippines.

413 In the study entitled "The earliest example of sexual dimorphism in bivalves —
414 evidence from the astartid *Nicaniella* (Lower Jurassic, southern Germany)," the
415 researchers utilized Principal Component Analysis and Fourier Analysis as a non-
416 invasive method that investigates sexual expression in the *Nicaniella rakoveci*. In
417 the study, researchers discovered that the bivalves with crenulations were found to
418 have a different shell shape, which made them more inflated than those without
419 crenulations. This suggests that when they became females, they adapted to
420 hold more eggs rather than for protection from predators as previously thought.
421 The formation of crenulations is likely part of the genetic process that controls
422 both the sex change and the changes in shell structure (Karapunar et al., 2021).
423 Overall, the findings demonstrate that the genetic mechanisms for sex change and
424 shell morphology in bivalves existed as early as the Early Jurassic, contributing
425 to our understanding of bivalve diversity and evolution. Thus, the researchers
426 concluded that crenulations serve as a morphological marker for identifying the
427 sex and reproductive stage of these bivalves (Karapunar et al., 2021).

428 On the other hand, invasive techniques such as histological analysis offer a
429 more thorough but harmful method for determining the sex of *T. granosa*. A
430 study on the Spawning Period of Blood Cockle *Tegillarca granosa* (Linnaeus,
431 1758) in Myeik Coastal. 240 blood cockle samples were examined for sex and
432 gonad maturity stages using histological examination, with shell lengths ranging
433 from 26–35mm and shell weights from 8.1–33g. For histological analysis, the whole
434 soft tissues were removed from the shell and the flesh containing most parts of
435 the gonads was fixed in formalin, dehydrated in an upgraded series of ethanol,
436 and cleared in xylene. This invasive method allows for precise identification of
437 the gonadal maturation stages based on the cellular and structural changes in the
438 gonads.

439 The classification of the gonad stages used was by Yurimoto et al. (2014).
440 There are five maturation stages of gonadal development: immature (Stage I),
441 developing (Stage II), mature (Stage III), spawning (Stage IV), and spent (Stage
442 V) stages. The sex of the *T. granosa* was confirmed by the color of the gonad and
443 by conducting a histological examination of the gonads. During the immature
444 stage, sex determination was indistinguishable due to the difficulties of observing
445 the germ cells. In the developing stage, the spermatocytes and a few spermatids
446 can be seen for males, and immature oocytes are attached to the tube wall for
447 the female. In the mature stage, the follicles are full of spermatozoa with their
448 tails pointing towards the center of the tube for the male, and the female is full
449 of mature oocytes that are irregular or polygonal in shape with the oval nucleus.
450 Upon reaching spawning, some spermatozoa are released, causing the empty space
451 in the follicle wall for males and females. There is a decrease in the number of
452 mature oocytes and it exhibits nuclear disappearance due to the breakdown of

453 the germinal vesicle. Lastly, the spent stage is where the genital tube is deformed
454 and devoid of spermatocytes which have completely spawned. In the female, the
455 genital tube is deformed and degenerated, making it empty. The morphology
456 of the cockle gonad shows that the area of the gonad increases according to the
457 increased levels of gonad maturity. The coloration of the gonad tissue layer in the
458 blood cockle varies from orange-red to pale orange in females and from white to
459 grayish-white in males for different maturity stages (May et al., 2021).

460 Although the histological examination is the most reliable method for obtaining
461 accurate information on the reproductive biology and sex determination of
462 *T. granosa*, it has limitations. Given its invasive nature, this approach requires
463 the dissection and destruction of specimens, making it unsuitable for continuous
464 monitoring and conservation efforts. Moreover, the current understanding of sex
465 determination in bivalves and mollusks is poor, and no chromosomes that can
466 be differentiated based on their morphology have been discovered (Afiati, 2007).
467 There exists a study that can provide insight into the sex-determining factor in
468 bivalves but *N. schoberti* is more difficult to analyze concerning potential sexual
469 dimorphism. Thickening the edges of the shell increases its inflation, which means
470 the shell can hold more space inside. This extra space helps protandrous females
471 accommodate more eggs.

472 **2.3 Machine Learning and Deep Learning in Bi- 473 ological Studies**

474 Machine learning has the potential to improve the quality of life of human beings
475 and has a wide range of applications in terms of research and development. The
476 term machine learning refers to the invention and algorithm evaluation that en-
477 ables pattern recognition, classification, and prediction based on models generated
478 from available data (Tarcă, Carey, Chen, Romero, & Drăghici, 2007). The study
479 of machine learning methods has advanced in the last several years, including bio-
480 logical studies. In biological studies, machine learning has been used for discovery
481 and prediction. This section will explore existing machine learning studies that
482 are applied in biological sciences, highlighting the identification of sex in shells,
483 bivalves, and mollusks.

484 **2.3.1 Deep Learning for Phenotype Classification in Ark
485 Shells**

486 In the study, the researchers utilized three (3) convolutional neural network (CNN)
487 models: the Visual Geometry Group Network (VGGnet), the Inception Residual
488 Network (ResNet), and the SqueezeNet (Kim, Yang, Cha, Jung, & Kim, 2024).
489 These deep learning models are utilized for the ark shells, namely *Anadara kagoshimensis*,
490 *Tegillarca granosa*, and *Anadara broughtonii*, to identify the phenotype
491 classification.

492 The researchers classified the ark shells based on radial rib count where they
493 investigated the difference in the number of radial ribs between three species and
494 were counted. Their CNN-based model that classifies images of three ark shells
495 can provide a theoretical basis for bivalve classification and enable the tracking of
496 the entire production process of ark shells from catching to selling with the support
497 of big data, which is useful for improving food safety, production efficiency, and
498 economic benefits (Kim et al., 2024).

499 **2.3.2 Geometric Morphometrics and Machine Learning for
500 Species Delimitation**

501 In *Geometric morphometrics and machine learning challenge currently accepted*
502 *species limits of the land snail Placostylus (Pulmonata: Bothriembryontidae)* on
503 *the Isle of Pines, New Caledonia*, the shell size was quantified using centroid size
504 from the Procrustes analysis, and both the shape and size information were used in
505 training the machine learning model. Their study concluded that the researchers
506 support utilizing both methods: supervised and unsupervised machine learning,
507 rather than choosing either of them individually. In general, their research con-
508 tributes to the growing number of studies that have combined geometric mor-
509 phometrics with the aid of machine learning, which is helpful in biological innovation
510 and breakthrough (Quenu, Trewick, Brescia, & Morgan-Richards, 2020).

511 **2.3.3 Contour Analysis in Mollusc Shells Using Machine
512 Learning**

513 Tuset et al. (2020), in their study, *Recognising mollusc shell contours with enlarged*
514 *spines: Wavelet vs Elliptic Fourier analyses*, mentioned that gastropod shells have
515 large spines and sharp shapes that differ based on environmental, taxonomic, and

516 evolutionary influences. The researchers stated that classic morphometric meth-
517 ods may not accurately depict morphological features of the shell, especially when
518 using the angular decomposition of the contour. The current research examined
519 and compared the robustness of the contour analysis using wavelet transformed
520 and Elliptic Fourier descriptors for gastropod shells with enlarged spines. For
521 that, the researchers analyzed two geographically and ecologically separated pop-
522 ulations of *Bolinus brandaris* from the NW Mediterranean Sea. Results showed
523 that contour analysis of gastropod shells with enlarged spines can be analyzed
524 using both methodologies, but the wavelet analysis provided better local discrim-
525 ination. From an ecological perspective, shells with various sizes of spines in both
526 areas indicate the broad adaptability of the species.

527 2.3.4 Machine Learning for Shape Analysis of Marine Or- 528 ganisms

529 In the study of Lishchenko and Jones (2021), titled *Application of Shape Analyses*
530 to *Recording Structures of Marine Organisms for Stock Discrimination and Taxo-*
531 *nomic Purposes*, they utilized geometric morphometrics (GM) as an approach to
532 the traditional method of collecting linear measurements with the application of
533 multivariate statistical methods and outline analysis in recording the structures
534 of marine organisms. The main taxonomic categories (mollusks, teleost fish, and
535 elasmobranchs) with their hard bodies have been used as an indication of age and
536 a determinable time-scale and structure continue to go through life (Arkhipkin,
537 2005; Kerr & Campana, 2014). This study has explored variations in the mor-
538 phometry of recording structures in stock discrimination and systematics. The
539 researchers utilized the principal component analysis rather than the traditional
540 approach, which helps simplify the data without losing important information.
541 They utilized landmark-based geometric morphometrics, which has three differ-
542 ent types, namely: discrete juxtaposition of tissue, maxima or curvature, or other
543 morphogenetic processes, and lastly, the extremal points are constructed land-
544 marks.

545 Generalized Procrustes Analysis (GPA) is a common superimposition tech-
546 nique in landmark-based geometric morphometrics that aligns landmarks via
547 translation, scaling, and rotation to eliminate non-shape deviations (Zelditch,
548 Swiderski, & Sheets, 2004). However, there is a limit to the amount of smooth
549 areas that may be captured, and it is possible to overlook significant shape details.
550 Utilization of the semi-landmarks enhanced the shape description (Adams, Rohlf,
551 & Slice, 2004). The researchers observed that using an outline-based approach
552 would be more effective than using a landmark-based approach.

553 Another approach is the Fourier analysis which is a curve-fitting approach
554 commonly used due to its well-known mathematical background and how general
555 functions can be decomposed into trigonometric or exponential functions with
556 definite frequencies. It has two main approaches, namely: Polar Transform (PT)
557 in which it expresses the outline using equally spaced radii, and Elliptical Fourier
558 Analysis (EFA) which separately analyzes the x and y coordinates of the shape.
559 The PT works for simple rounded outlines and has the tendency to miss details
560 in more complex shapes, unlike the EFA which can handle complex, convoluted
561 outlines (Zahn & Roskies, 1972; Doering & Ludwig, 1990; Ponton, 2006). Many
562 researchers view EFA as the most effective Fourier method for providing a compre-
563 hensive and detailed description of recording structures (Mérigot, Letourneau, &
564 Lecomte-Finiger, 2007; Ferguson, Ward, & Gillanders, 2011; Leguá, Plaza, Pérez,
565 & Arkhipkin, 2013; Mahé et al., 2016).

566 Landmark-based methods used in the study showed that there are detectable
567 differences between male and female octopuses. However, the accuracy of deter-
568 mining sex based on these differences was low, similar to the results obtained
569 with traditional morphometric techniques. The study involved a relatively small
570 sample size of 160 individuals, and the structure being analyzed (the stylet, or
571 internalized shell) varies significantly between individuals. Although the results
572 aligned with findings from other studies that attempted to identify gender differ-
573 ences in cephalopods, the researchers concluded that the approach might not be
574 accurate enough for reliable sex determination.

575 2.3.5 Deep Learning for Landmark-Free Morphological Fea- 576 ture Extraction

577 In another study, *a deep learning approach for morphological feature extraction*
578 *based on variational auto-encoder: an application to mandible shape*, the Morpho-
579 VAE machine learning approach was used to conduct a landmark-free shape ana-
580 lysis. Morpho-Vae reduces dimensions by concentrating on morphological features
581 that distinguish data with different labels using an image-based deep learning
582 framework that combines unsupervised and supervised machine learning. After
583 utilizing the method in primate mandible images, the morphological features re-
584 veal the characteristics to which family they belonged. Based on the result, the
585 method applied provides a versatile and promising tool for evaluating a wide range
586 of image data of biological shapes including those missing segments.

587 2.3.6 Machine Learning for Sex Differentiation in Abalone

588 In the study, *Towards Abalone Differentiation Through Machine Learning*, re-
589 searchers identified a problem in abalone farming which is having to identify the
590 sex of abalone to apply measures for its growth or preservation. The researchers
591 classified abalone sex using machine learning. Researchers trained the machine
592 to classify different types of classes which are male, female, and immature. The
593 results demonstrated the effectiveness of utilizing linear classifiers for this task.

594 Similarly, in the study, *Data scaling performance on various machine learning*
595 *algorithms to identify abalone sex*, the researchers of the University of India (2022)
596 focused on the data scaling performance of various machine learning algorithms to
597 identify the abalone sex, specifically using min-max normalization and zero-mean
598 standardization. The different machine learning algorithms are the Supervised
599 Vector Machine (SVM), Random Forest, Naive Bayesian, and Decision Tree. Their
600 study aims to utilize machine learning in terms of identifying the trends and
601 distribution patterns in the abalone dataset. Eight features of the abalone dataset
602 (length, diameter, height, whole weight, shucked weight, viscera weight, shell
603 weight, ring) were used to determine the three sexes of Abalone. Their data has
604 been grouped based on sex which are Female, Male, and Infant. They utilized
605 the Synthetic Minority Oversampling Technique (SMOTE) in data balancing for
606 the preprocessing of the data. Followed by data scaling or normalization where
607 it converts numeric values in a data set to a general scale without distorting
608 differences in the range of values. Then they classified by splitting the data into
609 training and testing sets (Arifin, Ariawan, Rosalia, Lukman, & Tufailah, 2021).

610 The study found that Naive Bayes consistently performed better than other al-
611 gorithms. However, when applied to both min-max and zero-mean normalization,
612 the average accuracies of the algorithms were as follows: Random Forest (62.37%),
613 SVM with RBF kernel (59.49%), Decision Tree (57.20%), SVM with linear ker-
614 nel (56.59%), and Naive Bayes (53.39%). Despite the performance decrease with
615 normalization, Random Forest achieved the highest overall metrics, including an
616 average balanced accuracy of 74.87%, sensitivity of 66.43%, and specificity of
617 83.31%. Liu et al. concluded that Random Forest is highly accurate because it
618 can handle large, complex datasets, run processes in parallel using multiple trees,
619 and select the most relevant features to enhance model performance (Arifin et al.,
620 2021).

621 **2.3.7 Machine Learning for Geographical Traceability in**
622 **Bivalves**

623 In the study, *BivalveNet: A hybrid deep neural network for common cockle (Cerastoderma edule) geographical traceability based on shell image analysis*, the re-
624 searchers incorporated computer vision and machine learning technologies for an
625 efficient determination of blood cockle harvesting origin based on the shell geomet-
626 ric and morphometric analysis. It aims to improve the traceability methodologies
627 in these organisms and its potential as a reliable traceability tool. Thirty *Cerasto-*
628 *derma edule* samples were collected along the five locations on the Atlantic West
629 and South Portuguese coast with individual images processed using lazy snapping
630 segmentation, spectro-textural-morphological phenotype extraction, and feature
631 selection through hybrid Principal Component Analysis and Neighborhood Com-
632 ponent Analysis (Concepcion, Guillermo, Tanner, Fonseca, & Duarte, 2023).

634 The researchers developed a non-invasive image-based traceability technique,
635 an alternative to the chemical and biochemical analysis of the bivalves. It was
636 able to incorporate machine learning methods to promote lesser human interven-
637 tion. The researchers discovered that BivalveNet emerged as the superior model
638 for bivalves with 96.91% accuracy which is comparable to the accuracy of the
639 destructive methods with 97% and 97.2% accuracy rates. The result of the study
640 aided the researchers in concluding that there is a possibility of on-site evalua-
641 tion of the bivalve through the implementation of a mobile app that would allow
642 the public and official entities to obtain information regarding the provenance of
643 seafood products' traceability because of its non-invasive and image-based aspects
644 (Concepcion et al., 2023).

645 *Tegillarca granosa* is known for having no sexual dimorphism. However, through
646 several related studies, the researchers can apply how family shells of *Tegillarca*
647 *granosa* have been identified based on its morphological and morphometric char-
648 acteristics and the methods used in machine learning in identifying its sex.

649 **2.4 Limitations on Sex Identification in *Tegillarca***
650 ***granosa***

651 To date, no distinction has been made between the male and female *T. granosa*
652 in sexing methodology. In cockle aquaculture without clearly apparent sexual
653 dimorphism, sexing can be performed using invasive methods such as chemical
654 stimulation, dissection, and gonad-stripping. Induced spawning, specifically tem-

655 perature shock, is the most natural and least invasive method for bivalves (Aji,
656 2011). However, the method (Wong & Lim, 2018) of immersing cockles in water
657 from hot to cold with a specific temperature requires deliberate and careful ma-
658 nipulation of the temperature over a specific period and would require constant
659 management and monitoring.

660 Recent studies involved non-invasive methods, with a specific emphasis on
661 morphological characteristics as indicators of sex differentiation. However, Tat-
662 suya Yurimoto et al. (2014) stated that the existing methods for determining
663 the sex of bivalves and mollusks in general are somewhat limited (Afiati, 2007).
664 At present, there is no recorded evidence of sexual dimorphism in *Tegillarca gra-*
665 *nosa*. Gonochoristic is the classification given to *Tegillarca granosa* (Lee, 1997).
666 However, Lee et al. (2012) reported that the sex ratio varied with shell length,
667 suggesting that sex might alter.

668 Hermaphrodites can exhibit either sequential (asynchronous) or simultaneous
669 (synchronous or functional) characteristics. Sequential hermaphrodites switch
670 genders after being male or female for one or multiple yearly cycles. (Heller,
671 1993; Gosling, 2004; Collin, 2013). Sex change and consecutive hermaphroditism
672 have been observed in different bivalve species, including Ostreidae, Pectinidae,
673 Veneridae, and Patellidae. However, macroscopically differentiating bivalve sex is
674 challenging. The only way it may be identified is through histological analysis of
675 gonad remains but to do so there is an act of killing the organism (Coe, 1943;
676 Gosling, 2004). Verification of sex change in bivalves to classify whether male or
677 female while they are alive is challenging since they need to be re-confirmed and
678 re-evaluated to be the same individual after a year.

679 Lee et al. (2012) found out that *T. granosa*, a species in Arcidae, has been
680 discovered to be a sequential hermaphrodite, with the sex ratio changing with an
681 increase in the shell size. In bivalves, sex changes usually happen when the gonad
682 is not differentiated between spawning seasons (Thompson, Newell, Kennedy, &
683 Mann, 1996). But in *T. granosa*, after the spawning season, sex changes during
684 its inactive phase. Results showed a 15.1% sex change ratio, with males having
685 a higher sex change ratio (21.2%) than females (6.2%). The 1+ year class had a
686 higher ratio (17.8%) than the 2+ year class (12.1%). Thus, this study indicates
687 that *T. granosa* is a sequential hermaphrodite. The results of the study demon-
688 strated that the bivalve's age affects the sex ratio and degree of sex change, but
689 additional in-depth investigation is required to determine the role that genetic
690 and environmental factors play in these changes.

691 No literature in the study of mollusks specifically addresses the machine learn-
692 ing algorithm used to determine the sex of *T. granosa* bivalves in various mod-
693 els. Nevertheless, various techniques such as shape analysis, morphometric ana-

694 lysis, Wavelet, and Fourier analysis, as well as different deep learning models like
695 VGNet, ResNet, and SqueezeNet in CNN networks, are utilized for phenotype
696 classification, while different machine learning algorithms could serve as the foun-
697 dation for this research project.

698 **2.5 Chapter Summary**

699 This section of the paper summarizes the technologies used in the different studies
700 related to the pursuit of the study entitled, Morphometric and Morphological-
701 Based Non-Invasive Sex Identification of Blood Cockles *Tegillarca granosa* (Lin-
702 naeus, 1758).

Author	Technology / Method Used	Description of Problem	Pros	Cons
D. V. Miranda and V. M. E. N. Ferriols	Temperature shock	No recent studies are available on the production and rearing of <i>T. granosa</i> in the Philippines.	Employed less invasive techniques which minimize the stress in <i>T. granosa</i> and can lead to better survival rates.	Time-consuming as the entire process from fertilization to the spat stage took 120 days.
Karapunar, Baran and Werner, W. and Fürsich, F. T. and Nützel, A.	Morphometric analysis, microscope imaging, principal component analysis (PCA), and Fourier shape analysis	To address the observed shell dimorphism in the Early Jurassic bivalve <i>Nicanella rakoveci</i> , namely the presence or lack of crenulations on the ventral shell margin, and whether these variations represent sexual dimorphism and sequential hermaphroditism.	The methods used reveal significant morphological differences with regard to sexual dimorphism.	There could be misinterpretation of the shape differences of bivalves due to the constraints and resolution of technologies used.
K. May and C. Maung and E. Phyu and N. Tun	Histological examination	The need to understand the reproductive period of <i>T. granosa</i> in Myeik to ensure sustainable aquaculture and to prevent overexploitation.	Method used allows for accurate sex identification based on the histological characteristics and color of the gonads.	Invasive technique used to determine the sex of <i>T. granosa</i> through gonad histological analysis.
E. Kim and S.-M. Yang and J.-E. Cha and D.-H. Jung and H.-Y. Kim	Convolutional neural network (CNN) models, VGGNet, Inception-ResNet, SqueezeNet	Traditional methods of recognizing and classifying ark shell species based on shell traits are time-consuming and inaccurate.	Automated classification of the three ark shells using a deep learning model obtained an accuracy of 92.4%.	Challenges may arise with certain ark shells that share similar morphology.
Mathieu Quemu and S. A. Trewick and F. Brescia and M. Morgan-Richards	Neural network analysis (supervised learning) and Gaussian mixture models (unsupervised learning)	To determine whether the shape and size of the snail's shells can distinguish between two <i>Placostylus</i> species, particularly in groups that appear to be hybrids.	Combining geometric morphometrics and machine learning effectively answers biological issues, providing insights into species classification and possible hybridization.	Difficulty classifying intermediate phenotypes, with potential for overfitting and misclassification in both learning methods.
V. M. Tusset and E. Galimany and A. Farrés and E. Marco-Herrero and J. L. Otero-Ferrer and A. Lombarte and M. Ramón	Wavelet functions and Elliptic Fourier descriptors	Addresses the difficulty of accurately defining phenotypic diversity in gastropod shells.	Advanced contour analysis methods allow accurate differentiation of gastropod shell forms.	Cannot clarify the causes of phenotypic variation in the two populations studied.
Fedor Lishchenko and Jones, J. B.	Landmark- and outline-based Geometric Morphometric methods	To address difficulties in differentiating between stocks of marine organisms to prevent misidentification that could affect conservation and management.	Shape analysis improves taxonomic classification precision and offers close distinction between related species or organisms.	Landmark-based methods can be sensitive to landmark placement.
M. Tsutsumi and N. Saito and D. Koyabu and C. Furusawa	Morphological regulated variational AutoEncoder (Morpho-VAE)	The need for reliable, landmark-free methods, such as a modified variational autoencoder, to extract and decipher complex shapes from image data.	Employs dimension reduction and feature extraction, making it a user-friendly tool for biology non-experts.	Limited sample size in certain families presented challenges.
Barrera-Hernandez, R. and Barrera-Soto, V. and Martinez-Rodriguez, J. L. and Ríos-Alvarado, A. B. and Ortiz-Rodriguez, F.	Machine learning algorithms	Identifying the sex of abalones is challenging for producers applying specific growth or preservation strategies.	Machine learning algorithms accurately classify abalone sex into three categories: male, female, and immature.	Selected features may not fully capture the complexity of abalone morphology.
Concepcion, R. and Guillermo, M. and Tanner, S. E. and Fonseca, V. and Duarte, B.	EfficientNet-Bo, ResNet101, MobileNetV2, InceptionV3	Addresses the difficulty of accurately tracing bivalve harvesting origins using computer vision and machine learning algorithms to enhance seafood traceability and combat food fraud.	Non-invasive, image-based tools for bivalve traceability provide faster, cheaper, and equally accurate alternatives to traditional chemical analysis methods.	Small sample size (only 30 cockles) limits model reliability.

Table 2.1: Comparison of the Methods Used in Bivalves Studies

703 Recent developments and breakthroughs in machine learning offer hopeful
704 solutions for biological issues. Research findings indicate that various machine
705 learning techniques such as CNNs, geometric morphometrics, and deep learning
706 models. They are deemed effective for identifying phenotypes and determining
707 the gender of various aquaculture commodities, such as mollusks and abalones.
708 These techniques provide a starting point for creating new, non-invasive ways to
709 differentiate male and female *T. granosa*, potentially addressing the drawbacks of
710 manual and invasive methods. Thus, machine learning to examine morphological
711 and morphometric features may streamline the process of sex identification.

712 Nevertheless, the use of machine learning to determine the sex of *T. granosa*
713 has not been fully explored. It lacks up-to-date and significant related literature
714 on using machine learning to identify sex in *T. granosa*, particularly given the
715 species' possible sequential hermaphroditism and lack of obvious external sexual
716 distinctions.

⁷¹⁷ **Chapter 3**

⁷¹⁸ **Research Methodology**

⁷¹⁹ This chapter discusses the materials and methods employed in the study, focusing
⁷²⁰ on the development requirements, as well as the software and programming
⁷²¹ languages utilized. It also detailed the overall workflow in conducting the study,
⁷²² Morphometric and Morphological-Based Non-Invasive Sex Identification of Blood
⁷²³ Cockles *Tegillarca granosa* (Linnaeus), 1758) using machine learning and deep
⁷²⁴ learning technologies.

⁷²⁵ Dr. Victor Emmanuel Ferriols, the director of the Institute of Aquaculture,
⁷²⁶ oversaw the overall workflow by providing baseline characteristics of the samples
⁷²⁷ that the researchers could focus on. Additionally, guidance was offered by the
⁷²⁸ research associates LC Mae Gasit and Allena Esther Artera. Consequently, the
⁷²⁹ entire dataset collection process was conducted at the University of the Philippines
⁷³⁰ Visayas hatchery facility.

⁷³¹ The methodology consisted of nine parts: (1) Sample Collection, (2) Ethical
⁷³² Considerations, (3) Creating *T.granosa* Dataset, (4) Morphological Characteris-
⁷³³ tics Collection (5) Image Acquisition and Pre-processing, (6) Hardware and Soft-
⁷³⁴ ware Configuration,(7) Morphometric Characteristics Evaluation Using Machine
⁷³⁵ Learning, (8) Morphological Characteristics Evaluation Using Deep Learning, and
⁷³⁶ (9) Evaluation Metrics

⁷³⁷ **3.1 Sample Collection**

⁷³⁸ The collection of *T. granosa* samples used in this study was part of an ongoing
⁷³⁹ research project by UPV DOST-PCAARRD titled "Establishment of the Center

740 for Mollusc Research and Development: Development of Spawning and Hatchery
741 Techniques for the Blood Cockle (*Anadara granosa*) for Sustainable Aquaculture.”
742 A total of 271 samples were provided for this study to classify the sex of *T. granosa*.
743 The samples, ranging in size from 34 to 61 mm, were sourced from the coastal area
744 of Zaraga, Iloilo, and fish markets in Ivisan, Capiz, Philippines (see Figure 3.1).

745 The research and experimentation were conducted at the University of the
746 Philippines Visayas hatchery facility in Miagao, Iloilo, where the samples were
747 maintained in 200 L fiberglass-reinforced plastic (FRP) tanks containing filtered
748 seawater with 35 ppt salinity (Miranda & Ferriols, 2023).

749 As part of the data collection process, the researchers utilized induced spawning
750 and dissection to classify the sex of the samples. Induced spawning through
751 temperature fluctuations was the most natural and least invasive method for bi-
752 valves compared to other approaches (Aji, 2011). However, since not all samples
753 exhibited gamete release, the researchers also performed dissections, assisted by
754 hatchery staff, to expedite data collection. The sex of the dissected samples was
755 identified based on the coloration of gonad tissue, which varies according to sex
756 and maturity stage. Females exhibited orange-red to pale orange gonads, while
757 males displayed white to grayish-white gonads (May et al., 2021).

758 The methods used for data collection were considered noninvasive, particularly
759 given that *T. granosa* are oxygen regulators well adapted to tidal exposure and
760 hypoxia (Davenport & Wong, 1986).

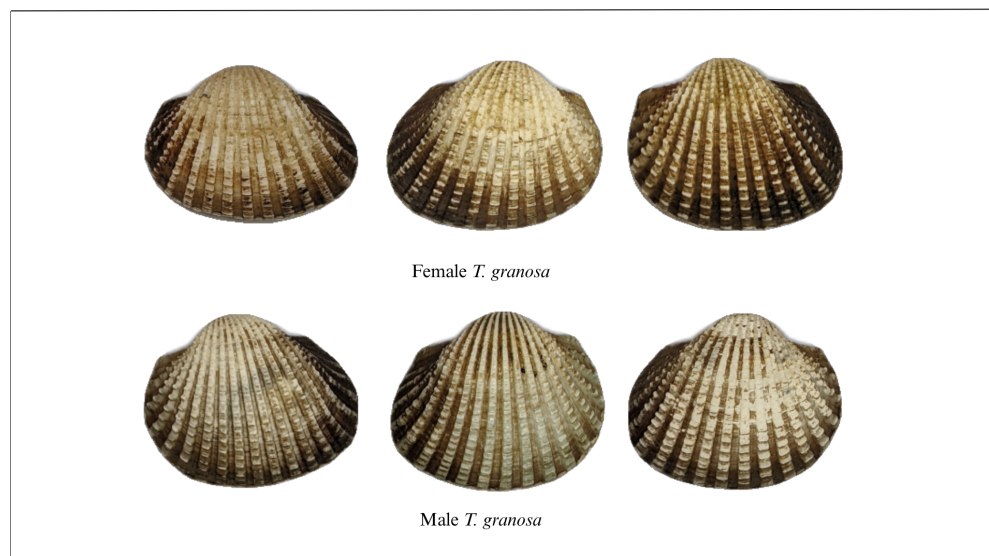


Figure 3.1: Male and Female *Tegillarca granosa* shells

761 3.2 Ethical Considerations

762 The ongoing research project titled "Establishment of the Center for Mollusc Re-
763 search and Development: Development of Spawning and Hatchery Techniques for
764 the Blood Cockle (*Anadara granosa*) for Sustainable Aquaculture"—from which
765 the samples used in this study were obtained—was reviewed and approved by the
766 Institutional Animal Care and Use Committee (IACUC) of the University of the
767 Philippines Visayas.

768 3.3 Creating *T. granosa* Dataset

769 The experiment began with the collection of preliminary observations from 100 *T.*
770 *granosa* samples. For the actual experimentation, the researchers collected the full
771 dataset in batches until a total sample size of 271 *T. granosa* was reached. Lin-
772 ear measurements—including width, height, length, rib count, hinge line length,
773 and the distance between the umbos—were recorded and organized into a CSV
774 file. This dataset served as the foundation for training and testing machine learn-
775 ing models, as well as for establishing a baseline for the Convolutional Neural
776 Networks.

777 Images of each sample were captured and saved in JPG format using a stan-
778 dardized file naming convention that included the sample's sex, the shell's ori-
779 entation or view, and its corresponding number out of the 271 total samples. File
780 names for female *T. granosa* samples began with "0", while those for male sam-
781 ples began with "1". Each file name also included one of the six captured views:
782 (1) dorsal, (2) ventral, (3) anterior, (4) posterior, (5) left lateral, and (6) right
783 lateral (refer to Figure 3.2), followed by a unique sample number. For exam-
784 ple, "010001" denoted the first female sample taken from the dorsal view, while
785 "110001" represented the first male sample from the same view. This naming
786 convention was implemented to prevent data leakage and ensure accurate labeling
787 of images according to their respective samples.

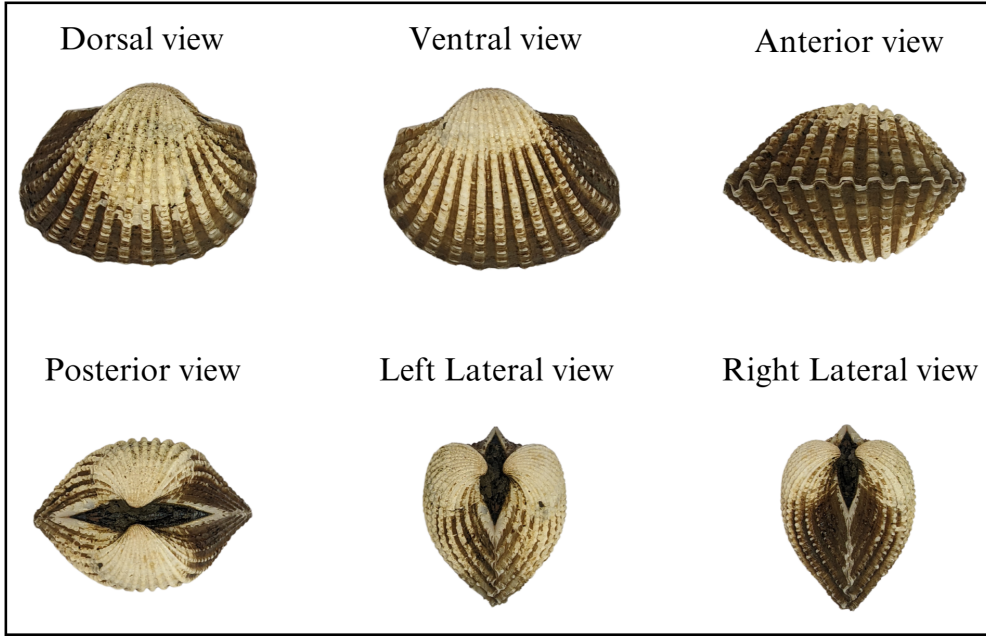


Figure 3.2: Different Views of the *T. granosa* Shell Captured

⁷⁸⁸ 3.4 Morphometric and Morphological Characteristics Collection

⁷⁹⁰ Morphology refers to biological form and is one of the most visually recognizable
⁷⁹¹ phenotypes across all organisms (Tsutsumi, Saito, Koyabu, & Furusawa, 2023).
⁷⁹² In this study, morphological characteristics describe the structural features of
⁷⁹³ *T. granosa*, focusing on measurable attributes such as shape, size, and color.
⁷⁹⁴ Morphometric characteristics, on the other hand, refer to specific quantifiable
⁷⁹⁵ features of *T. granosa*, including length, width, height, hinge line length, distance
⁷⁹⁶ between the umbos, and rib count. As stated by the researchers, quantifying and
⁷⁹⁷ characterizing these traits is essential for understanding and visualizing variations
⁷⁹⁸ in *T. granosa* morphology.

⁷⁹⁹ The researchers measured the height, width, and length of *T. granosa* using
⁸⁰⁰ a Vernier caliper with a precision of up to 0.01 mm. Refer to Figure 3.3 for the
⁸⁰¹ corresponding measurement diagram. Length (A) refers to the distance from the
⁸⁰² anterior to the posterior of the shell. Width (B) is defined as the widest span
⁸⁰³ across the shell from the left to the right valve. Height (C) measures the distance
⁸⁰⁴ from the base to the apex of the shell. In addition, the hinge line length (D) near
⁸⁰⁵ the hinge and the distance between the umbos (E) were recorded.

⁸⁰⁶ Reyment and Kennedy (1998) emphasized that including rib count as supple-

807 mentary information can enhance identification accuracy. Following this insight,
808 the researchers also recorded the rib count for both male and female *T. granosa*,
809 adjusting the values by calculating ratios to account for natural size variation
810 among specimens.

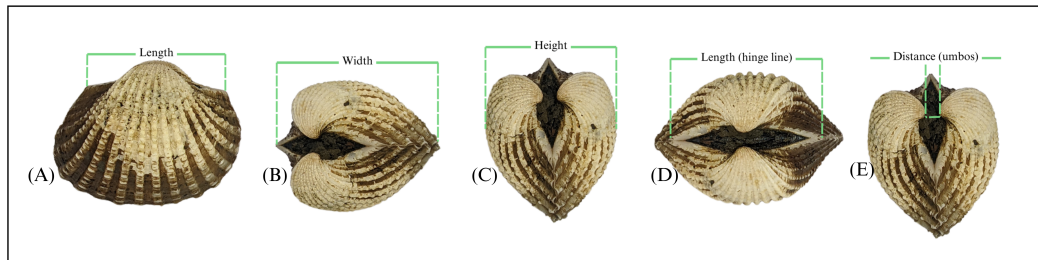


Figure 3.3: Linear Measurements of *Tegillarca granosa* shell.

811 3.5 Image Acquisition and Data Gathering

812 This study comprised 144 male and 127 female *T. granosa* samples, resulting
813 in a total of 1,626 images captured from various angles. To ensure consistency
814 during image acquisition, the researchers constructed a box-like structure with
815 a white background to control the imaging environment. This setup allowed for
816 uniform image captures by fixing the camera at a consistent angle directly above
817 the *T. granosa*. A ring light was positioned in front of the box to enhance image
818 quality, eliminate shadows, and ensure clarity of the samples throughout the image
819 acquisition process.

820 The images were captured using a Google Pixel 3 XL smartphone, which fea-
821 tures a resolution of 2960×1440 pixels and a 12.2 MP camera (4032×3024 pix-
822 els). Additional camera specifications include an f/1.8 aperture, 28mm wide lens,
823 $\frac{1}{2.55}$ " sensor size, $1.4\mu\text{m}$ pixel size, dual-pixel phase detection autofocus (PDAF),
824 and optical image stabilization (OIS) (Concepcion et al., 2023).



Figure 3.4: Image Acquisition Setup for *T. granosa* Samples

825 3.6 Hardware and Software Configuration

826 This section of the paper discusses the software, programming languages, and tools
827 used for sex identification. Data collection, preprocessing, and model training
828 were conducted on a Windows 11 operating system using an ACER Aspire 3
829 general-purpose unit (GPU) equipped with an AMD Ryzen 3 7320U CPU with
830 Radeon Graphics (8 cores) @ 2.395 GHz and 8 GB of RAM. Google Colaboratory
831 was utilized for collaborative preprocessing, computer vision tasks, and model
832 training. Image preprocessing was performed using computer vision techniques in
833 Python, while machine learning and deep learning models were developed using
834 Python libraries, including Keras. The results of the gathered measurements were
835 stored and managed using spreadsheet software. GitHub was employed for version
836 control, documentation, and activity tracking throughout the study.

837 3.7 Morphometric Characteristics Evaluation Us- 838 ing Machine Learning

839 This section of the paper discusses the machine learning operations that served
840 as a baseline prior to implementing more complex deep learning methods for
841 image classification. The study utilized collected variables including linear mea-
842 surements—length, width, height, hinge line length, distance between the um-
843 bos, and rib count—along with derived features used as predictors. These in-
844 cluded the length-to-width ratio, length-to-height ratio, width-to-height ratio,
845 umbo distance-to-length ratio, hinge line length-to-length ratio, umbo distance-

846 to-height ratio, and rib density. The samples were classified by sex, with females
847 labeled as 0 and males as 1, which served as the response variable.

848 **3.7.1 Data Preprocessing**

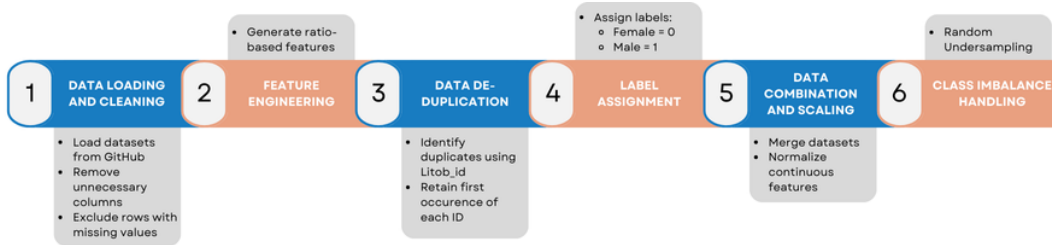


Figure 3.5: Data Preprocessing Pipeline

849 The preprocessing of the dataset involved several essential steps, carried out
850 using Python in Google Colaboratory, in preparation for machine learning analysis
851 (see Figure 3.5).

852 ***Data Loading and Cleaning***

853 The process began by loading two separate datasets for male and female *T.
854 granosa* directly from GitHub using `pd.read_csv()`. Unnecessary columns were
855 removed, and rows containing missing values were excluded using the `dropna()`
856 function to ensure data completeness and reliability.

857 ***Feature Engineering***

858 Additional ratio-based features were generated to augment the existing mea-
859 surements. These included the length-to-width ratio, length-to-height ratio, width-
860 to-height ratio, hinge line length-to-length ratio, umbos distance-to-length ratio,
861 umbos distance-to-height ratio, and rib density. These derived features aimed to
862 emphasize shape characteristics independent of size, improving the models' ability
863 to distinguish morphological differences between sexes.

864 ***Data De-duplication***

865 To avoid redundancy and ensure each specimen was uniquely represented, the
866 last three digits of each `Litob_id` were used to identify duplicates. Only the first
867 occurrence of each unique ID was retained, reducing potential bias caused by
868 repeated entries.

869 ***Label Assignment***

870 A new column labeled `Label` was added to both datasets. Female specimens
871 were assigned a label of 0, and male specimens a label of 1. This column served
872 as the target variable for classification.

873 ***Data Combination and Scaling***

874 After cleaning and feature engineering, the male and female datasets were
875 merged into a single DataFrame. The `Litob_id` column was removed post de-
876 duplication. All continuous numeric features were normalized using `MinMaxScaler`
877 to scale values to the range [0, 1].

878 Rib count was excluded from normalization because it is a discrete feature with
879 biologically meaningful bounds. According to best practices in machine learning,
880 normalizing discrete or categorical features can distort their meaning and is often
881 unnecessary (Jaiswal, 2024). In this study, rib count was treated as a categorical
882 attribute due to its biological significance and finite, non-continuous nature.

883 ***Class Imbalance Handling***

884 After normalization, class imbalance was addressed by applying Random Under-
885 sampling to the male dataset. This technique randomly reduced the number of
886 male samples to match the number of female samples (127 each), ensuring equal
887 class representation. By using this approach, model bias was minimized, and the
888 classification performance became more reliable across both classes.

889 **3.7.2 Machine Learning Models Training**

890 ***Model Selection and Hyperparameter Tuning***

891 To establish a baseline for classification, various models were evaluated: Logis-
892 tic Regression, K-Nearest Neighbors, Support Vector Machine, Random Forest,
893 AdaBoost, Extra Trees, and Gradient Boosting. Hyperparameter tuning was con-
894 ducted using `GridSearchCV`, which systematically identified the optimal settings
895 for each model to enhance accuracy and performance.

896 ***Cross-Validation***

897 A five-fold cross-validation approach was implemented. The dataset was di-
898 vided into five subsets, with four used for training and one for testing. This
899 process was repeated five times, with each fold serving as the test set once. This

900 method ensured that model evaluation was robust and generalizable, minimizing
901 the bias that may result from a single train-test split. (GeeksforGeeks, 2024)

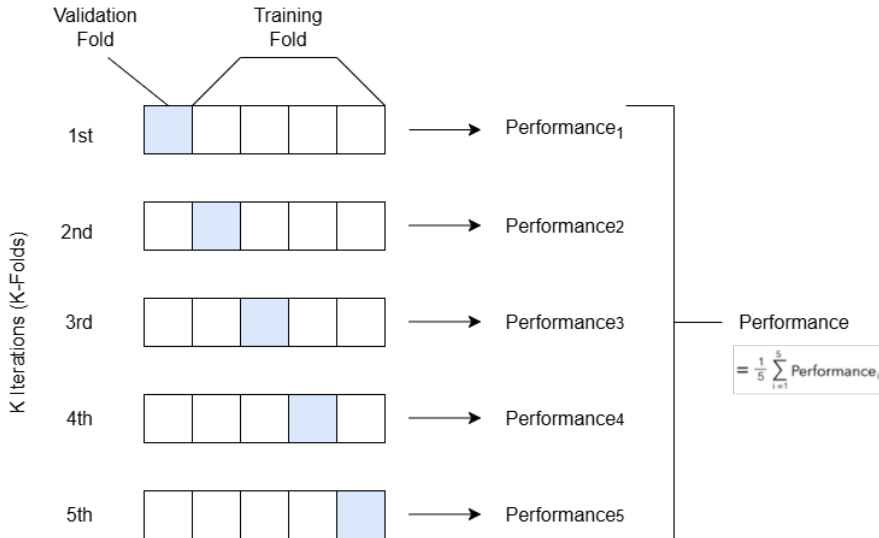


Figure 3.6: Diagram of k-fold cross-validation with $k = 5$

902 3.8 Morphological Characteristics Evaluation Us- 903 ing Deep Learning

904 This section outlines the application of deep learning techniques in analyzing the
905 morphological characteristics of *Tegillarca granosa* to identify their sex based on
906 shell images. A Convolutional Neural Network (CNN) architecture was imple-
907 mented and trained on preprocessed images using stratified cross-validation.

908 *Image Preprocessing*

909 This subsection details the image processing techniques applied to raw shell
910 images of *T. granosa* using computer vision methods before training the deep
911 learning model. The image preprocessing techniques include standardizing input
912 dimensions and removing shadows, background, and noise. Each image under-
913 went data augmentation to enhance feature visibility for effective learning. Image
914 preprocessing ensures consistent and high-quality input data for model training.

915 *Adjusting Dimensions*

916 All images were resized to a consistent dimension of 256x256 pixels to ensure
917 uniformity throughout the dataset. This standardization is essential for Convo-

918 lutional Neural Networks (CNNs), as a consistent input dimension is required.
919 While resizing, the aspect ratio was maintained to prevent distortion of the mor-
920 phological features, and padding was added to retain the original format.

921 ***Background Removal***

922 Background removal was performed to maintain a consistent white background
923 throughout the dataset. The tool `rembg` was used to efficiently remove the original
924 background, retaining the foreground from the raw images. This method resulted
925 in clear images with a white background, enhancing focus on the morphological
926 features and defining the shell boundaries.

927 ***Shadow Removal***

928 To minimize noise caused by shadows around the shell, HSV thresholding,
929 contours, and morphological thresholds were applied to isolate and remove shad-
930 owed regions. This approach preserved the natural color of the blood cockles and
931 eliminated shadows and noise from the surrounding area.

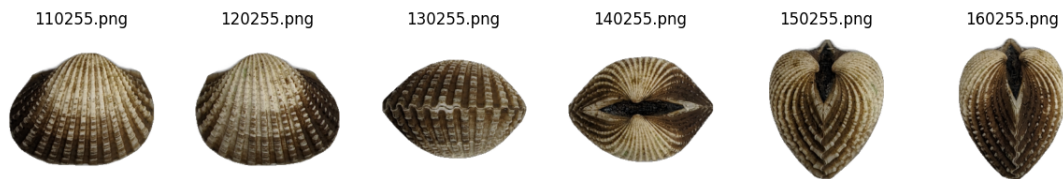


Figure 3.7: Shadows removed from male samples at different angles

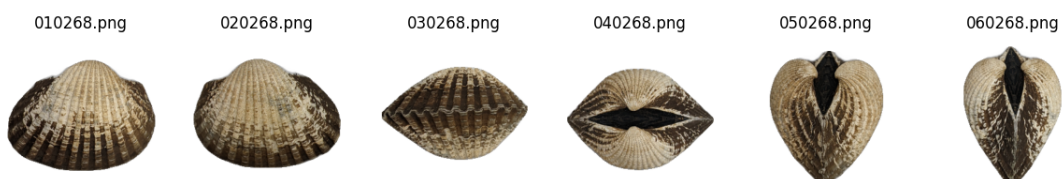


Figure 3.8: Shadows removed from female samples at different angles

932 **3.8.1 Convolutional Neural Network**

933 Convolutional Neural Networks are the main deep learning tool used in image
934 classification, specifically binary classification. CNNs leverage their ability to
935 share weights and use pooling techniques, reducing the number of parameters (Cui,
936 Pan, Chen, & Zou, 2020). The proposed CNN architecture for sex identification
937 of blood cockles employs 12 layers designed to extract features from the input

938 image with dimensions. The layers consist of four convolution layers, a flatten
 939 layer, dropout and two dense layers. The CNN framework used in this study is
 940 shown in Figure 3.9.

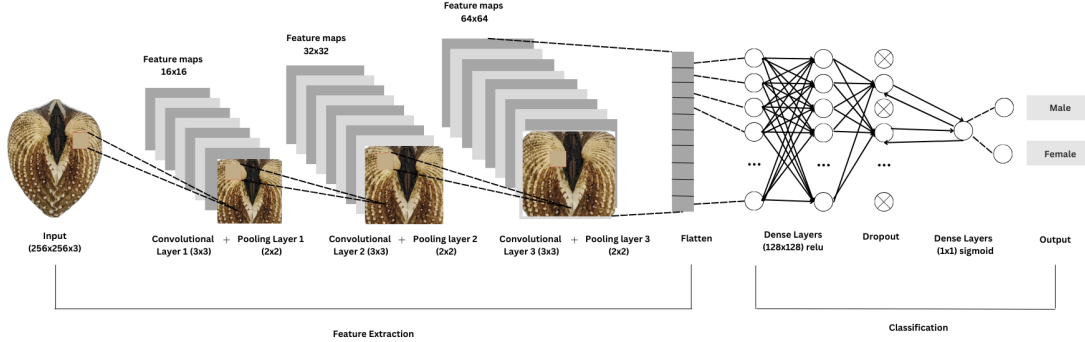


Figure 3.9: Architecture of Convolutional Neural Network (CNN)

941 ***Convolution Layer***

942 The convolution layers of CNN extract the features from the input image
 943 through the convolution operation. This study uses four convolution layers with
 944 a 3x3 kernel size and filter sizes of 16, 32, 64, and 128. The first layer extracts
 945 the low-level features, such as edges, lines, and corners, while the deeper layers
 946 iteratively extract more complex information from these low-level features. The
 947 ReLU activation function is used as the baseline for this model, and experiments
 948 are conducted with different activation functions, such as ELU and PReLU, to
 949 evaluate their impact on learning complex patterns within the data.

950 ***Pooling Layer***

951 A pooling layer was added after the convolution layer to enhance calculation
 952 speed and prevent overfitting (Cui et al., 2020). In this study, max pooling was
 953 applied with a (3,3) kernel size.

954 ***Fully Connected and Dropout***

955 Fully connected layers follow after the convolution and pooling layers. Each
 956 neuron connects to all neurons of the previous layer. The output values from the
 957 fully connected layers are sent to an output layer. It was classified using different
 958 sigmoid functions appropriate for binary classification.

959 A large number of parameters in the training process can lead to overfitting.
 960 It occurs when the model learns the training data too well, including its noise and
 961 irrelevant details. This results in poor performance on unseen data. To mitigate
 962 the overfitting, the dropout layer was employed. Dropout works by temporarily

963 discarding a portion of the neurons in the network with probability p ($0 < p < 1$).
964 During this process, these neurons do not participate in the forward propagation
965 process of CNN and the backward propagation process (Cui et al., 2020).

966 **3.8.2 CNN Training**

967 The dataset consists of 1626 samples, with 127 samples from females and 144 samples
968 from males, individually for each angle. Given the minimal class imbalance,
969 random undersampling was carried out to create a balanced dataset. All images
970 were resized to 256x256 pixels and normalized using a Rescaling layer, ensuring
971 pixel values were within the range [0, 1].

972 ***Data Splitting***

973 Due to the limited dataset size, a traditional train-test split was not adopted.
974 Instead, a 5-fold stratified cross-validation approach was used to maximize the
975 use of available data while preserving the class distribution within each fold.
976 `StratifiedKFold` was applied to ensure that the distribution of male and female
977 samples remained consistent across all folds, thereby enabling fair and robust
978 model evaluation (GeeksforGeeks, 2020).

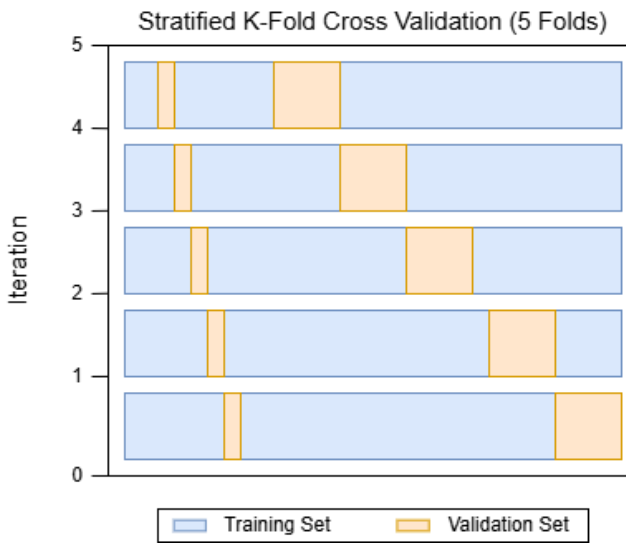


Figure 3.10: Diagram of stratified k-fold cross-validation with $k=5$

979 ***Data Augmentation***

980 Before model training, online data augmentation was applied exclusively to
981 the training data within each fold, creating new data variations on the fly. The

982 augmentations included random horizontal flips, slight rotations, and zoom trans-
983 formations to enhance data diversity and improve model generalization (Awan,
984 2022). All augmentation was strictly applied only to the training subset of each
985 fold to prevent data leakage and maintain the validity of the results (*Figure 3.11*).

986 On-the-fly data augmentation (OnDAT) generates augmented data during
987 each iteration, exposing the model to constantly changing data variations. Aug-
988 menting the original data allows better exploration of the underlying data genera-
989 tion process and has the potential to prevent the model from overfitting spurious
990 patterns, thereby improving performance (Cerqueira, Santos, Baghoussi, & Soares,
991 2024).

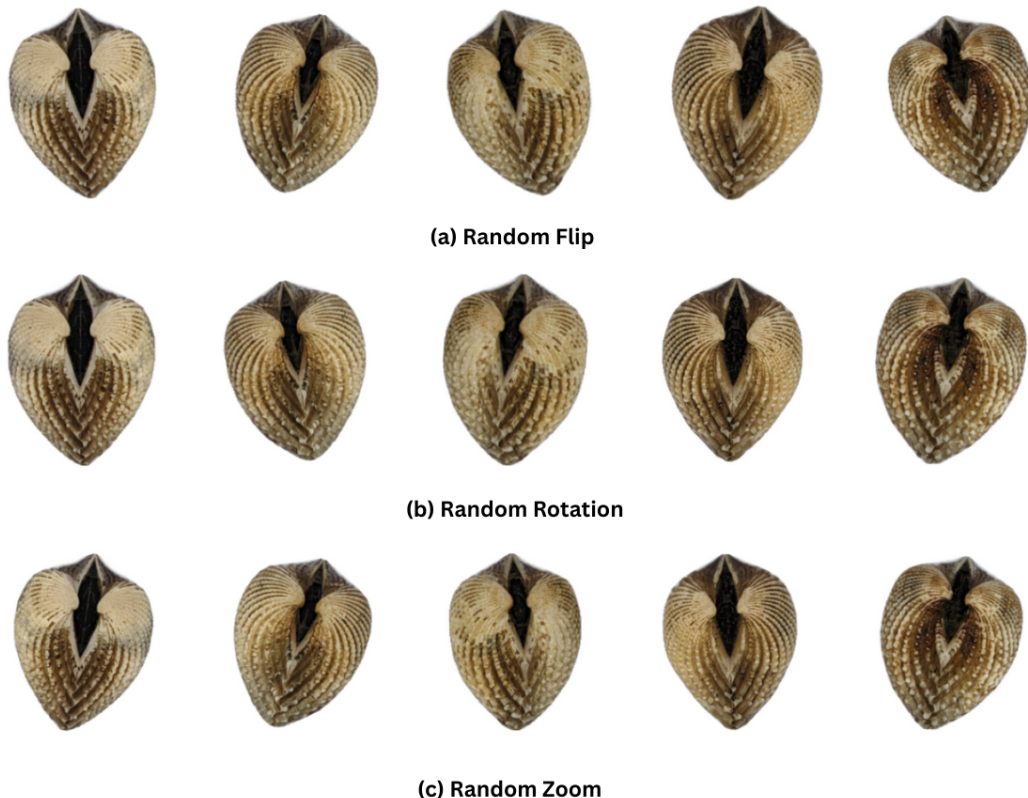


Figure 3.11: Data Augmentation Techniques

992 ***Training Procedure***

993 During the training process, model performance per fold was carefully mon-
994 itored. One important thing to observe is the consistency in the performance,
995 whether the model is still learning or is at high risk of overfitting. Early stopping
996 was applied to ensure the stable performance of the model across folds. This
997 technique allows for monitoring the training of the neural network, stopping when

998 the performance metrics, in this case, validation loss, cease to improve. Further-
999 more, to enhance the learning process, `ReduceLROnPlateau` was applied, which
1000 decreased the learning rate if there was no improvement in the model for a speci-
1001 fied number of epochs (Team, n.d.).

1002 The model was trained using the Adam optimization algorithm, with an ini-
1003 tial learning rate of 0.001. Binary cross-entropy, commonly known as the log loss,
1004 was employed as the loss function due to its effectiveness in binary classifica-
1005 tion tasks. To reduce the risk of overfitting, a dropout rate of 0.5 was applied, ran-
1006 domly deactivating half of the neurons during the training process to improve
1007 generalization.

1008 3.9 Evaluation Metrics

1009 Evaluating the performance of a binary classification model is essential, and se-
1010 lecting appropriate metrics depends on the specific requirements of the user. The
1011 performance of both supervised machine learning and deep learning models will
1012 be measured using several key metrics, including accuracy, precision, recall, F1
1013 score, and the AUC-ROC score.

1014 Accuracy (ACC) is the ratio of the overall correctly predicted samples to the
1015 total number of examples in the evaluation dataset (Cui et al., 2020). It measures
1016 the overall correctness of the model in predicting both male and female blood
1017 cockles. This metric provides insight into how well the model performs across all
1018 classifications. The formula for accuracy is:

$$1019 \text{ACC} = \frac{\text{Correctly classified samples}}{\text{All samples}} = \frac{TP + TN}{TP + FP + TN + FN} \quad (3.1)$$

1019 Precision (PREC) is the ratio of correctly predicted positive samples to all
1020 samples assigned to the positive class (Cui et al., 2020). This metric helps in
1021 evaluating the fairness of the model and prevents the misclassification of blood
1022 cockles as it identifies potential inaccuracies or biases. The formula for precision
1023 is:

$$1024 \text{PREC} = \frac{\text{True positive samples}}{\text{Samples assigned to positive class}} = \frac{TP}{TP + FP} \quad (3.2)$$

1024 Recall (REC), also known as sensitivity or the true positive rate (TPR), is the

ratio of correctly predicted positive cases to all the actual positive samples (Cui et al., 2020). It represents the ability of the model to correctly identify positive male and female samples. The formula for recall is:

$$\text{REC} = \frac{\text{True positive samples}}{\text{Samples classified positive}} = \frac{TP}{TP + FN} \quad (3.3)$$

The F1 score is the harmonic mean of precision and recall, which penalizes extreme values of either of the two metrics (Cui et al., 2020). It is particularly useful when the class distribution is imbalanced. The formula for the F1 score is:

$$F1 = \frac{2 \times \text{precision} \times \text{recall}}{\text{precision} + \text{recall}} = \frac{2 \times TP}{2 \times TP + FP + FN} \quad (3.4)$$

The Area Under the Receiver Operating Characteristic Curve (AUC-ROC) is a performance measurement for classification problems, particularly used in deep learning in this study. The ROC curve is a plot of the true positive rate (recall) against the false positive rate (1 - specificity), and the AUC score quantifies the overall ability of the model to discriminate between positive and negative classes. A higher AUC indicates better model performance. (Nahm, 2022)

¹⁰³⁷ **Chapter 4**

¹⁰³⁸ **Results and Discussions**

¹⁰³⁹ This chapter presents the results from the machine learning and deep learning
¹⁰⁴⁰ analyses conducted on the preprocessed dataset. It includes an evaluation of
¹⁰⁴¹ various machine learning classifiers and the application of deep learning models
¹⁰⁴² for image-based classification. The primary focus is on identifying key predictors
¹⁰⁴³ and assessing classification performance for sex identification in *T. granosa*.

¹⁰⁴⁴ **4.1 Machine Learning Analysis**

¹⁰⁴⁵ This chapter outlines the results of preprocessing, training of machine learning
¹⁰⁴⁶ models, and feature importance analysis, all conducted in Google Colab using
¹⁰⁴⁷ Python. The dataset was preprocessed in Colab, and the training and evaluation
¹⁰⁴⁸ of various classifiers were performed entirely within this environment. This part of
¹⁰⁴⁹ the paper includes five subsections: data exploration, statistical analysis, feature
¹⁰⁵⁰ importance analysis, performance evaluation, and confusion matrix analysis.

¹⁰⁵¹ **4.1.1 Data Exploration**

¹⁰⁵² Exploratory data analysis was performed to characterize the dataset using visu-
¹⁰⁵³ alizations to understand the patterns and correlations within the data. A corre-
¹⁰⁵⁴ lation heatmap was created to assess the relationship between the predictors and
¹⁰⁵⁵ the target variable.

¹⁰⁵⁶ The heatmap (see Figure 4.1) revealed three features most correlated with the

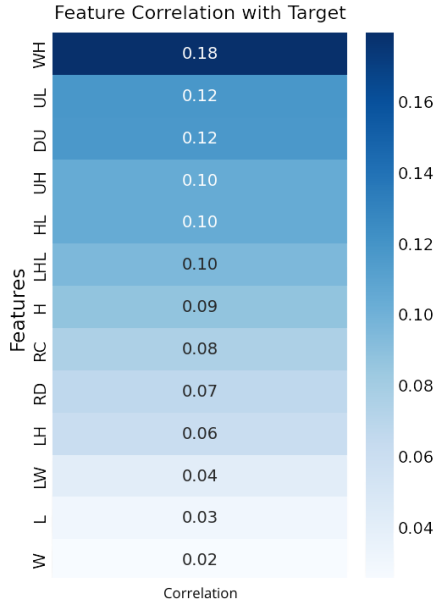


Figure 4.1: Correlation heatmap of morphometric features with the sex of *T. granosa*

1057 sex of *T. granosa*: the width-height ratio ($r = 0.18$), the umbos-length ratio ($r = 0.12$), and the distance between the umbos ($r = 0.12$). Each of these features
 1058 demonstrated a weak positive relationship with the target variable.
 1059

1060 4.1.2 Statistical Analysis

1061 As part of the exploratory data analysis, statistical testing confirmed that the
 1062 dataset did not follow a normal distribution (see Table 4.1). Consequently, the
 1063 Mann-Whitney U test was applied with a significance level of $\alpha = 0.05$ to com-
 1064 pare male and female samples. Out of thirteen features, five showed statistically
 1065 significant differences. These included: distance between umbos ($p = 0.025$),
 1066 length-width ratio ($p = 0.011$), umbos-length ratio ($p = 0.019$), width-height
 1067 ratio ($p = 0.003$), and umbos-height ratio ($p = 0.036$).

1068 It is important to note that statistical significance does not imply predictive
 1069 importance. Therefore, further analysis, such as feature importance evaluation,
 1070 was performed to identify the most informative predictors for classification.

Variable	p-value
WH_ratio	0.003
LW_ratio	0.011
UL_ratio	0.019
Distance Umbos	0.025
UH_ratio	0.036
HL_ratio	0.079
Length (Hinge Line)	0.120
Height	0.124
Rib Density	0.181
Rib count	0.251
Length	0.334
LH_ratio	0.490
Width	0.753

Table 4.1: Mann-Whitney U Test Results for Sex-Based Feature Comparison

¹⁰⁷¹ 4.1.3 Feature Importance Analysis

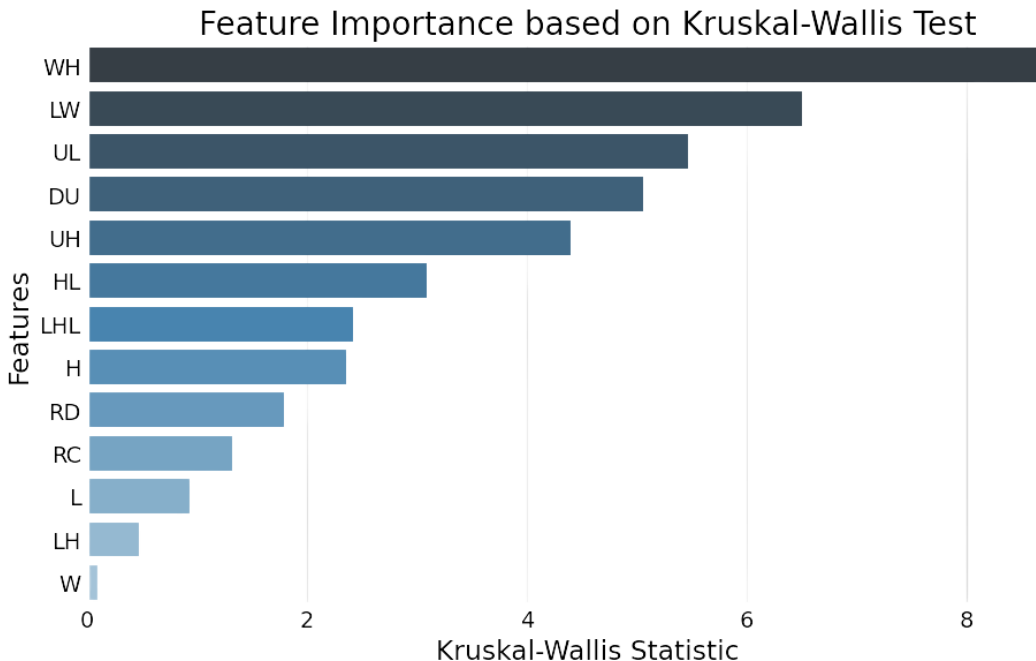


Figure 4.2: Feature Importance Scores Using the Kruskal-Wallis Test

¹⁰⁷² Feature importance was assessed using the Kruskal-Wallis test, a non-parametric
¹⁰⁷³ method that is suitable for evaluating differences in distributions across groups

1074 when the data does not follow a normal distribution. This approach was chosen
 1075 because of the non-normality of the dataset and its robustness in handling con-
 1076 tinuous and ordinal data without assuming homogeneity of variances. (Ribeiro,
 1077 2024)

1078 The analysis showed that the width-to-height ratio (WH ratio) had the high-
 1079 est importance score, indicating it is the most statistically significant feature for
 1080 distinguishing the sex of *T. granosa*. Other notable features included the length-
 1081 to-width ratio (LW ratio), umbo distance-to-length ratio (UL ratio), distance
 1082 between the umbos, and umbo distance-to-height ratio (UH ratio), all of which
 1083 contributed significantly to the classification task.

1084 4.1.4 Performance Evaluation

Model	Accuracy (%)	Precision (%)	Recall (%)	F1-Score (%)
Support Vector Machine	58.62	58.62	58.62	58.44
Logistic Regression	57.83	57.83	57.83	57.61
K-Nearest Neighbors	51.18	51.31	51.18	50.77
Extra Trees	59.07	59.54	59.07	58.45
Random Forest	59.85	59.99	59.85	59.80
Gradient Boosting	61.03	61.32	61.03	60.81
AdaBoost	60.63	60.98	60.63	60.39

Table 4.2: Performance Metrics for Models with All 13 Features

1085 Table 4.2 shows the performance metrics of different machine learning models
 1086 trained using all 13 features from the dataset. Among the models, Gradient
 1087 Boosting achieved the highest accuracy of 61.03%, along with strong precision,
 1088 recall, and F1-score values. AdaBoost also performed competitively, with an ac-
 1089 curacy of 60.63%. These results highlight the effectiveness of ensemble methods
 1090 such as Gradient Boosting and AdaBoost when utilizing the full feature set, likely
 1091 because of their capability to combine multiple weak learners into a more robust
 1092 predictive model (Hussain & Zaidi, 2024).

Model	Accuracy (%)	Precision (%)	Recall (%)	F1-Score (%)
Support Vector Machine	63.77	64.47	63.77	63.42
Logistic Regression	63.75	63.87	63.75	63.70
K-Nearest Neighbors	64.16	64.97	64.16	63.75
Extra Trees	61.04	61.68	61.04	60.67
Random Forest	61.01	61.12	61.01	60.91
Gradient Boosting	64.15	64.24	64.15	64.01
AdaBoost	61.02	61.26	61.02	60.82

Table 4.3: Performance Metrics for Models with 5 Features

1093 Table 4.3 presents the performance of the same models using only the top
1094 five features identified through Kruskal-Wallis feature importance analysis. The
1095 selected features are the distance between the umbos, length-to-width ratio, width-
1096 to-height ratio, umbo distance-to-height ratio, and umbo distance-to-length ratio.

1097 Interestingly, the overall performance of the models improved when using only
1098 the top 5 features compared to using all 13. K-Nearest Neighbors (KNN) achieved
1099 the best results with an accuracy of 64.16%, precision of 64.97%, recall of 64.16%,
1100 and an F1-score of 63.75%. Gradient Boosting followed closely behind. These find-
1101 ings suggest that reducing the feature set to the most relevant variables helped
1102 simplify the models, improved generalization, and enhanced predictive perfor-
1103 mance—particularly for KNN, which showed a notable improvement over its ear-
1104 lier results with the full feature set.

1105 **4.1.5 Confusion Matrix Analysis**

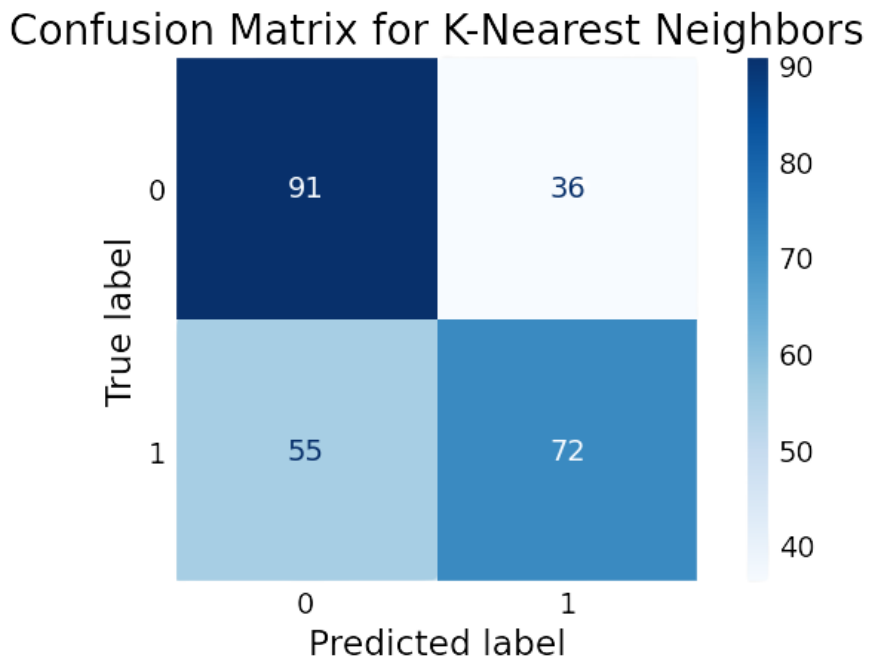


Figure 4.3: Feature Importance Scores Using the Kruskal-Wallis Test

1106 Figure 4.3 summarizes the performance of the K-Nearest Neighbors model in
1107 classifying *T. granosa* based on their sex, where 0 represents female samples and
1108 1 represents male samples. From the matrix, we observe that out of all the actual
1109 female samples (true label 0), 91 were correctly predicted as female (true positive
1110 for class 0), while 36 were incorrectly classified as male (false negative for class

1111 0). On the other hand, out of all the actual male samples (true label 1), 72 were
1112 correctly predicted as male (true positive for class 1), while 55 were incorrectly
1113 classified as female (false negative for class 1).

1114 4.2 Deep Learning Analysis

1115 This section presents the performance of the Convolutional Neural Network (CNN)
1116 model in classifying the sex of *T. granosa* based on shell morphology. The analysis
1117 evaluates the model's ability to distinguish between male and female shell images
1118 using various evaluation metrics. This part of the paper includes six subsections:
1119 baseline model, comparison of individual and combined angles, training result and
1120 hyperparameter tuning, proposed model, learning rates and training behavior per
1121 fold, and visualizations.

1122 The machine learning analysis (see Figure 4.3) revealed that five of the origi-
1123 nal features produced significant results. The K-Nearest Neighbor (KNN) model
1124 achieved an accuracy of 64.16%, precision of 64.97%, recall of 64.16%, and an F1
1125 score of 63.75%. This section compares the model's performance across differ-
1126 ent angles based on the results of the machine learning and feature importance
1127 analysis.

1128 4.2.1 Baseline Model

1129 This section presents the baseline model with a batch size of 16 and 20 epochs,
1130 which will serve as the starting point for comparison and provide a guideline for
1131 hyperparameter tuning. The focus will be on one of the angles, specifically the
1132 Left Lateral view, since the feature importance analysis using the Kruskal-Wallis
1133 Test indicated that the width-to-height ratio had the highest importance score,
1134 which is most visible from the Left Lateral view.

Dataset	Accuracy (%)	Precision (%)	Recall (%)	F1-Score (%)	AUC score (%)	Loss (%)
Unbalanced	65.27	71.82	58.99	63.99	73.08	0.6122
Balanced	67.34	69.43	64.06	65.60	74.31	0.5981

Table 4.4: Performance Metrics for Unbalanced vs. Balanced Datasets (Batch Size: 16, Epochs: 20)

1135 The unbalanced dataset, which consisted of 144 male samples and 127 female
1136 samples, achieved an accuracy of 65.27%, precision of 71.82%, recall of 58.99%,

1137 an F1-score of 63.99%, an AUC score of 73.08%, and a loss of 0.6122. However, to
 1138 address the class imbalance and enhance model performance, random undersam-
 1139 pling was performed. This approach resulted in improved performance metrics for
 1140 the balanced dataset, with an accuracy of 67.34%, precision of 69.43%, a recall
 1141 of 64.06%, an F1-score of 65.60%, an AUC score of 74.31%, and a lower loss of
 1142 0.5981.

1143 **4.2.2 Comparison of Individual and Combined Angles**

1144 Using the same batch size and number of epochs, performance was compared
 1145 across all individual angles and the combination of the two highest-performing
 1146 angles based on accuracy, using a balanced dataset. For the combined analysis,
 1147 samples from the two selected angles were placed side by side, and a new dataset
 1148 folder was created for male and female samples.

Angle	Accuracy (%)	Precision (%)	Recall (%)	F1-Score (%)	AUC score (%)	Loss (%)
Dorsal	66.54	63.76	77.88	69.96	73.09	0.6152
Ventral	67.30	69.33	66.18	66.53	74.87	0.6159
Anterior	51.57	31.11	6.31	10.02	65.87	0.6825
Posterior	61.43	63.48	51.17	54.25	70.12	0.6257
Left Lateral	67.34	69.43	64.06	65.60	74.31	0.5981
Right Lateral	65.37	67.18	59.82	62.99	71.02	0.6115
Ventral + Left Lateral	62.60	67.02	57.85	58.57	70.37	0.6433

Table 4.5: Performance Metrics for Individual and Combined Angles (Batch Size: 16, Epochs: 20)

1149 Table 4.5 presents the performance metrics for each individual angle and the
 1150 combination of the two highest-performing angles in terms of accuracy. The
 1151 Left Lateral view achieved the highest accuracy (67.34%) and precision (69.43%),
 1152 while the Dorsal view obtained the highest recall (77.88%) and F1-score (69.96%).
 1153 Meanwhile, the Ventral view recorded the highest AUC score (74.87%), indicat-
 1154 ing its strong ability to distinguish between classes. Combining the Ventral and
 1155 Left Lateral views resulted in an overall accuracy of 62.60%, suggesting that while
 1156 combined images may provide complementary information, individual angle views
 1157 still outperformed the combined views under the current experimental setup.

1158 **4.2.3 Training Result and Hyperparameter Tuning**

1159 The Left Lateral angle was selected for further optimization. Several experiments
 1160 were conducted by tuning hyperparameters such as batch size, number of epochs,

and activation functions. Each adjustment was compared against the baseline model to enhance performance and develop a robust CNN for sex classification of *T. granosa*.

The Left Lateral angle was chosen because it achieved the highest accuracy and precision among all individual views, and because the Kruskal-Wallis feature importance analysis indicated that the width-to-height ratio, a feature most visible from the lateral perspective, was the most significant morphological trait for classification. Therefore, focusing on this view was expected to maximize the model's learning capacity and improve classification performance.

A. Batch Size and Number of Epochs

Batch Size	No. of Epoch	Accuracy (%)	Precision (%)	Recall (%)	F1-Score (%)	AUC score (%)	Loss (%)
16	20	67.34	69.43	64.06	65.60	74.31	0.5981
16	30	67.73	70.17	64.06	65.72	75.76	0.5900
16	50	67.73	70.17	64.06	65.72	75.76	0.5900
32	20	68.13	72.25	58.95	62.34	74.76	0.6041
32	30	71.28	73.17	66.89	68.27	76.76	0.5832
32	50	71.68	72.52	69.29	69.12	77.34	0.5824
64	20	56.71	65.96	36.83	41.46	71.28	0.6692
64	30	57.95	61.94	48.12	52.66	71.22	0.6241
64	50	61.10	62.68	56.12	56.83	73.46	0.6086

Table 4.6: Effect of Batch Size and Epoch Values on CNN Model Performance

Table 4.6 shows the results indicating that a batch size of 32 with 50 epochs achieved the best overall performance, with an accuracy of 71.68%, a precision of 72.52%, a recall of 69.29%, an F1-score of 69.12%, and AUC score of 77.34%.

In contrast, increasing the batch size to 64 resulted in lower recall and F1-scores, suggesting that smaller batch Sizes (16 or 32) are more effective for this dataset. A moderate batch size of 32 allowed the model to generalize better and maintain stable learning, while too large batch sizes may have led to underfitting.

B. Activation Functions

Activation Functions	Accuracy (%)	Precision (%)	Recall (%)	F1-Score (%)	AUC score (%)	Loss (%)
ReLU	71.68	72.52	69.29	69.12	77.34	0.5824
ELU	53.14	32.91	53.08	39.95	58.23	0.6796
PreLU	62.64	66.59	50.43	56.96	72.33	0.6162

Table 4.7: Performance Metrics for Different Activation Functions (Batch Size: 32, Epochs: 50)

Table 4.7 the performance of different activation functions applied to the CNN model trained with a batch size of 32 and 50 epochs. Based on the results, the

1181 ReLU activation function achieved the best overall performance, with an accuracy
1182 of 71.68%, precision of 72.52%, recall of 69.29%, F1-score of 69.12%, and
1183 AUC score of 77.34%, along with the lowest loss at 0.5824. This suggests that
1184 ReLU remains an effective activation function for the classification of *T. granosa*,
1185 outperforming both ELU and PReLU in this setup.

1186 4.2.4 Proposed Model

1187 This section presents the performance evaluation of the proposed Convolutional
1188 Neural Network (CNN) model, trained with a batch size of 32, 50 epochs, and using
1189 the ReLU activation function. The model's effectiveness was assessed through
1190 5-fold cross-validation to ensure robustness and generalizability across different
1191 data partitions.

Fold no.	Accuracy (%)	Precision (%)	Recall (%)	F1-Score (%)	AUC score (%)	Loss (%)
Fold 1	76.47	70.59	92.31	80.00	73.08	0.5975
Fold 2	62.75	70.59	46.15	55.81	71.85	0.6202
Fold 3	78.43	75.00	84.00	79.25	84.92	0.5392
Fold 4	62.75	71.43	40.00	51.28	71.08	0.6331
Fold 5	78.00	75.00	84.00	79.25	85.76	0.5219

Table 4.8: Per-Fold Performance Metrics (Batch Size: 32, Epochs: 50, Activation Function: ReLU)

1192 The proposed model consistently achieved high performance in Folds 1, 3, and
1193 5, with accuracies above 76% and strong recall and AUC scores, demonstrating
1194 its potential for reliable sex identification of *T. granosa*. The slight variation
1195 in performance across folds may be attributed to differences in data distribution,
1196 emphasizing the importance of further data augmentation and balancing for future
1197 work.

1198 4.2.5 Learning Rates and Training Behavior per Fold

1199 This section presents the learning rate adjustments, early stopping events, and
1200 best epoch selections for each fold during the 5-fold cross-validation of the pro-
1201 posed model. During training, the ReduceLROnPlateau callback was employed
1202 to monitor the validation loss and automatically reduce the learning rate when
1203 performance plateaued. Additionally, EarlyStopping was utilized to halt training
1204 once no further improvement was observed after a set patience, and the model
1205 weights were restored from the end of the best-performing epoch to ensure optimal
1206 performance.

1207 The following table summarizes the epochs where learning rate reductions
 1208 occurred, the adjusted learning rates, the epochs at which early stopping took
 1209 place, and the best epochs from which model weights were restored for each fold.

Fold no.	Epoch (LR Reduced)	Learning Rate After Reduction	Early Stopping Epoch	Best Epoch (Restored)
Fold 1	20	0.0005000	25	17
	23	0.0002500		
Fold 2	9	0.0005000	19	11
	14	0.0002500		
	17	0.0001250		
Fold 3	15	0.0005000	20	12
	18	0.0002500		
Fold 4	12	0.0005000	32	24
	15	0.0002500		
	27	0.0001250		
	30	0.0000625		
Fold 5	20	0.0005000	25	17
	23	0.0002500		

Table 4.9: Learning Rate Reductions, Early Stopping, and Best Epochs per Fold During 5-Fold Cross-Validation

1210 4.2.6 Visualizations

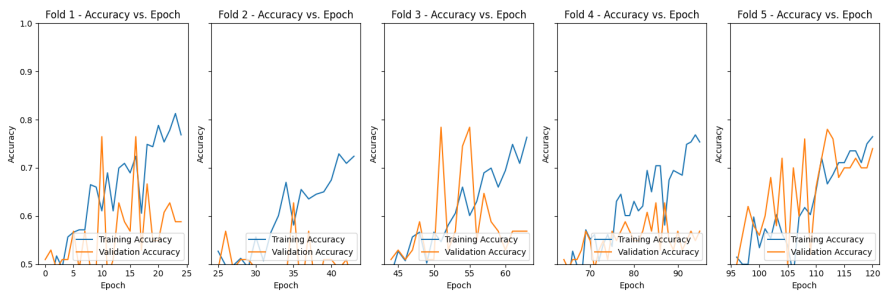


Figure 4.4: Training and Validation Accuracy per Fold

1211 Figure 4.4 shows the performance of the model in the training and validation
 1212 in terms of accuracy across five folds. The graph across folds displays a consistent
 1213 upward trend for the training accuracy. However, there is an observable change in
 1214 the performance, particularly in Folds 1 and 2, where it shows a slight downward
 1215 trend in the validation accuracy.

1216 Figure 4.5 shows the average performance of the model in both training and

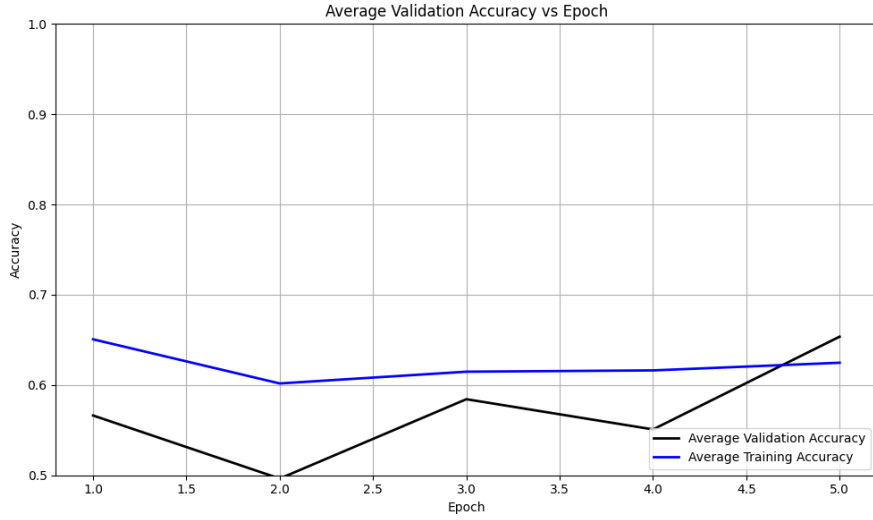


Figure 4.5: Average Training and Validation Accuracy Across Folds

accuracy in terms of accuracy across five folds. Similar to the individual performances, there is an observable upward trend, which shows that the accuracy score improves with the number of folds. The validation accuracy shows a downward and upward trend that shows that it gradually improves on later epochs. The accuracy in the training is slightly higher than the accuracy when validating the model, it indicates that the model learns during training.

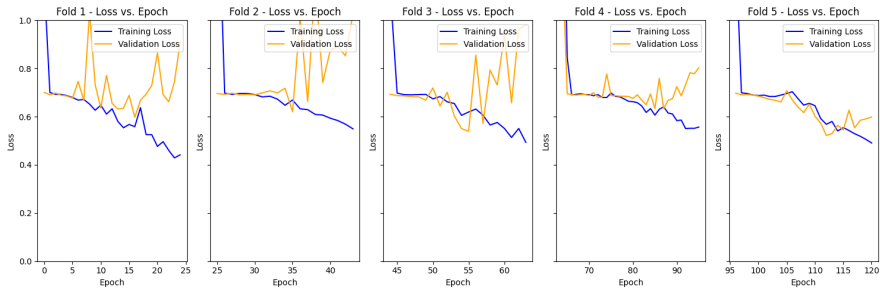


Figure 4.6: Training and Validation Loss per Fold

Figure 4.6 shows the performance of the model in the training and validation in terms of the training and validation loss across five folds. The graph across folds displays a consistent downward trend for the training loss. On the other hand, there is an observable change in the performance, especially in Folds 1,2,3, and 4, where it shows an upward trend in the validation loss. This is an implication for the learning performance of the model, as it may not be learning effectively.

Figure 4.7 shows the average performance of the model in both the training and validation in terms of loss across five folds. There is an observable downward trend

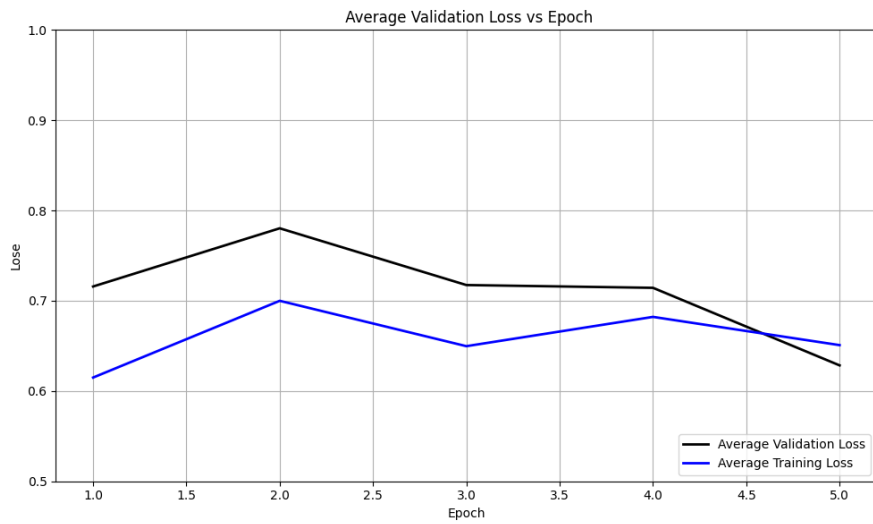


Figure 4.7: Average Training and Validation Loss Across Folds

in both the average loss for training and validation. Additionally, the average training loss is slightly lower than the average validation loss.

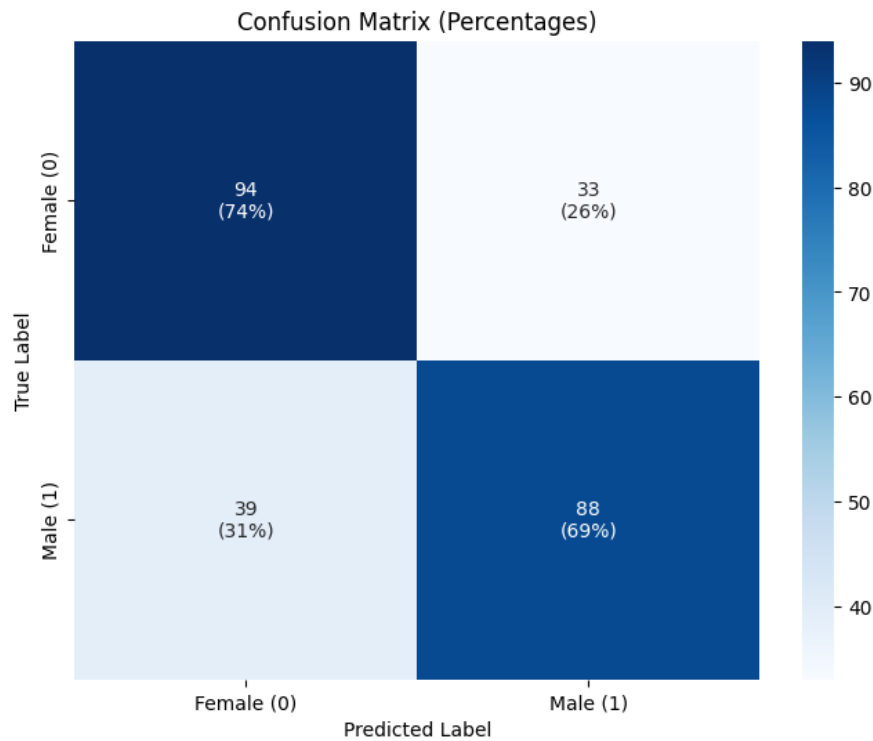


Figure 4.8: Confusion Matrix for Final Model Predictions

1233 Figure 4.8 shows the confusion matrix for the true class label and predicted
1234 class label. The matrix shows the correctly predicted male and female samples
1235 along with their corresponding percentages. There is an observable trend where
1236 females have slightly higher true positives compared to males in the number and
1237 percentages for the correctly classified male and female samples, which are 94 and
1238 88, corresponding to 74% and 69%, respectively. Additionally, the false classified
1239 samples were 33 for females and 39 for males, respectively accounting for 26% and
1240 31%.

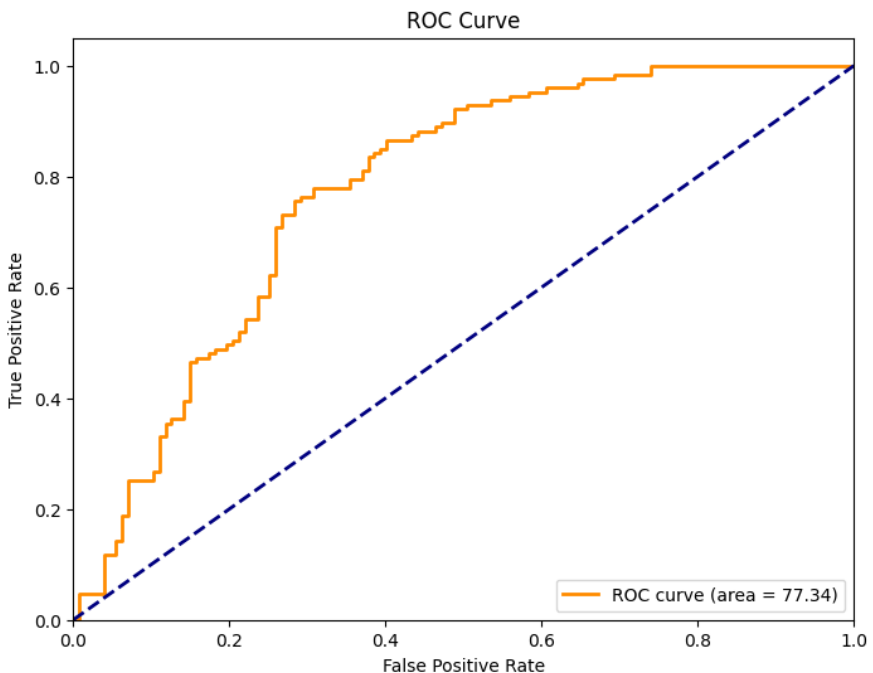


Figure 4.9: ROC Curve and AUC Score

1241 Figure 4.9 shows the ROC Curve shows the ability of the proposed model to
1242 correctly identify the true positives, which can help determine the tradeoff between
1243 specificity and sensitivity. It will also determine the validity of the model, that it is
1244 not predicting based only on random chances. The range of AUC ROC is between
1245 0.5 and 1. The model was able to achieve a score of 0.7734, which is better than
1246 random chances and an indication that the model is performing reasonably.

1247 4.3 Discussions

1248 This study aimed to develop a non-invasive method for identifying the sex of *T.*
1249 *granosa* using machine learning, deep learning, and computer vision technologies.

1250 The dataset was manually curated by the researchers, including both the linear
1251 measurements and the images captured from six different angles.

1252 The machine learning approach revealed that using five key features, selected
1253 through statistical tests (Mann-Whitney U-test and Kruskal-Wallis test), out-
1254 performed models trained on all 13 features. The K-nearest neighbors (KNN)
1255 classifier, using only these five features, achieved an accuracy of 64.16%, precision
1256 of 64.97%, recall of 64.16%, and an F1-score of 63.57%. These results indicate
1257 that a more focused set of features can enhance model performance, confirming
1258 the potential of non-invasive sex identification using linear measurements.

1259 Further deep learning experiments explored how different image angles im-
1260 pacted performance. The study found that the Left Lateral view consistently
1261 produced the best results, with an accuracy of 71.68%, precision of 72.52%, recall
1262 of 69.29%, F1-score of 69.12%, and an AUC score of 77.34%. This suggests that
1263 optimizing image angles is crucial, and combining multiple angles did not signif-
1264 icantly improve the model's performance. Data augmentation and regularization
1265 techniques, such as early stopping, helped improve the model's generalization and
1266 prevent overfitting.

1267 The findings are significant because they demonstrate the feasibility of a non-
1268 invasive, accurate, and efficient sex identification method for *T. granosa*. This
1269 approach aligns with sustainable aquaculture practices by reducing the need for
1270 harmful physical sex-identifying methods. By integrating machine learning with
1271 deep learning image analysis, this study provides a valuable model for non-invasive
1272 sex identification which could be applied to other species in aquaculture as well.

1273 When compared to similar existing studies such as the gender classification
1274 method for Chinese mitten crab using deep learning CNN (Cui *et al.*, 2020), there
1275 are notable differences in methodology. The crab study used grayscale images and
1276 a CNN with three convolutional layers, achieving 98.90% accuracy. In contrast,
1277 this study utilized a hybrid approach combining machine learning with deep learn-
1278 ing CNNs, trained on RGB images (256×256), and a deeper CNN architecture.
1279 Despite achieving lower accuracy (71.68%), this variation could be due to the sub-
1280 tler morphological differences between male and female *T. granosa*, or possibly
1281 due to image quality limitations and sample size.

1282 There are limitations in this study, particularly the size of the dataset (271
1283 samples) and the reliance on six fixed image angles. These constraints may not
1284 fully represent the morphological variability across different populations or en-
1285 vironments. Despite these limitations, the study successfully demonstrates that
1286 combining machine learning and deep learning with computer vision can provide
1287 a reliable and non-invasive solution for sex identification in *T. granosa*.

₁₂₈₈ **Chapter 5**

₁₂₈₉ **Conclusion and**
₁₂₉₀ **Recommendations**

₁₂₉₁ **5.1 Conclusion**

₁₂₉₂ This study utilized the application of machine learning and deep learning tech-
₁₂₉₃ niques to identify the sex of *T. granosa* based on the morphometric characteristics.
₁₂₉₄ A manually curated dataset was developed, consisting of both linear measurements
₁₂₉₅ and images captured from six different angles. Machine learning methods were
₁₂₉₆ employed to identify statistically significant features, which served as the basis for
₁₂₉₇ deep learning analysis using a 12-layer Convolutional Neural Network (CNN). The
₁₂₉₈ proposed CNN model yielded an average accuracy of 71.68% in the performance
₁₂₉₉ metrics. Overall, this study offers a classification approach which is a viable so-
₁₃₀₀ lution for non-invasive sex identification, providing an in-depth analysis based on
₁₃₀₁ *T. granosa*'s linear measurements and morphological characteristics from different
₁₃₀₂ angles.

₁₃₀₃ Through the availability of the gathered data, trial-and-error experimentation
₁₃₀₄ was conducted by adjusting the number of layers, batch size, epoch, and activa-
₁₃₀₅ tion functions. The different combinations tested provided baseline results that
₁₃₀₆ demonstrate the feasibility of non-invasive sex identification for *T. granosa*.

₁₃₀₇ While the study has made significant progress, challenges were encountered
₁₃₀₈ during CNN training, particularly due to hardware memory limitations. To over-
₁₃₀₉ come these, the researchers utilized synchronous Google Colab with 100 comput-
₁₃₁₀ ing units, requiring subscriptions, repeated retraining, and reconfigurations, which
₁₃₁₁ demanded considerable financial resources and time to optimize the parameters.

Upon comparing the experimental results of model parameters, it was demonstrated that non-invasive sex identification on *T. granosa* is achievable through the integration of machine learning and deep learning methods. Machine learning models based on five statistically selected features had better performances than those based on all features, with an accuracy of 64.16%, precision of 64.97%, recall of 64.16%, and an F1-score of 63.57% using K-nearest neighbors (KNN) classifier. The classification performance was further enhanced by deep learning models, using Left Lateral image view, achieving an accuracy of 71.68%, precision of 72.52%, recall of 69.29%, F1-score of 69.12%, and an AUC score of 77.34%.

These findings establish that the CNN model can serve as a baseline for future studies on non-invasive sex identification of *T. granosa* and potentially other similar species. By providing a practical and less harmful alternative to traditional methods, this research contributes a significant advancement in the field of aquaculture and marine biology.

5.2 Recommendations

This special problem entitled Morphometric and Morphological-Based Non-invasive Sex Identification of *T. granosa* focuses on creating a baseline study that will serve as a foundation for further studies involving *T. granosa*, blood cockles, using machine learning, computer vision, and deep technologies in determining the sex of the samples is a salient need in aquaculture practices. Thus, the proposed recommendations are the future applications to improve and have detailed analysis, such as focusing on shape analysis, exploring other state-of-the-art deep learning techniques, or transfer learning, such as ResNet, SqueezeNet, and InceptionNet, and comparing the analysis results. Furthermore, the main goal of conducting this is to have the ability to identify the sex of the samples by taking real-time angles by rotating from the dorsal, lateral, and ventral.

Due to the time constraints, the researchers were only able to gather a total of 1,626 images with 271 images per angle, and utilized these for model training and validation. A larger and more diverse collection of images could further improve the model's generalization. In order to capture more variability, future study might include expanding the dataset to improve classification performance.

Future studies could also invest in a sturdier and more controlled environment by using a green background and positioning a fixed camera angle during image acquisition. In addition, researchers may experiment with other image processing techniques such as morphological transformations to emphasize features. The

₁₃₄₇ dataset can be utilized for further analysis through advanced deep learning and
₁₃₄₈ computer vision methods to make sense of the images gathered and discern sexual
₁₃₄₉ dimorphism for *T. granosa* .

¹³⁵⁰ References

- 1351 Adams, D. C., Rohlf, F. J., & Slice, D. E. (2004). Geometric morphometrics: ten
1352 years of progress following the ‘revolution’. *Italian Journal of Zoology*, *71*,
1353 5–16. doi: 10.1080/11250000409356545
- 1354 Afifiati, N. (2007, 01). Gonad maturation of two intertidal blood clams anadara
1355 granosa (l.) and anadara antiquata (l.) (bivalvia: Arcidae) in central java. ,
1356 *10*.
- 1357 Aji, L. P. (2011). Review: Spawning induction in bivalve. *Jurnal Penelitian
1358 Sains*, *14*, 14207.
- 1359 Arifin, W. A., Ariawan, I., Rosalia, A. A., Lukman, L., & Tufailah, N. (2021).
1360 Data scaling performance on various machine learning algorithms to identify
1361 abalone sex. *Jurnal Teknologi Dan Sistem Komputer*, *10*(1), 26–31. doi:
1362 10.14710/jtsiskom.2021.14105
- 1363 Arkhipkin, A. I. (2005). Statoliths as ‘black boxes’ (life recorders) in squid.
1364 *Marine and Freshwater Research*, *56*, 573–583. doi: 10.1071/mf04158
- 1365 Awan, A. A. (2022, November). *A complete guide to data augmentation*. Retrieved from <https://www.datacamp.com/tutorial/complete-guide-data-augmentation>
- 1366 Aypa, S. M., & Baconguis, S. R. (2000). Philippines: mangrove-friendly aquacul-
1367 ture. In J. H. Primavera, L. M. B. Garcia, M. T. Castaños, & M. B. Sur-
1368 tida (Eds.), *Mangrove-friendly aquaculture: Proceedings of the workshop on
1369 mangrove-friendly aquaculture organized by the seafdec aquaculture depart-
1370 ment, january 11-15, 1999, iloilo city, philippines* (pp. 41–56).
- 1371 BFAR. (2019). *Philippine fisheries profile 2018* (Tech. Rep.). PCA Compound,
1372 Elliptical Road, Quezon City, Philippines: Bureau of Fisheries and Aquatic
1373 Resources.
- 1374 Boey, P.-L., Maniam, G. P., Hamid, S. A., & Ali, D. M. H. (2011). Utilization of
1375 waste cockle shell (anadara granosa) in biodiesel production from palm olein:
1376 Optimization using response surface methodology. *Fuel*, *90*(7), 2353–2358.
1377 doi: 10.1016/j.fuel.2011.03.002
- 1378 Breton, S., Capt, C., Guerra, D., & Stewart, D. (2017, June). *Sex determining
1379 mechanisms in bivalves*. Preprints.org. doi: 10.20944/preprints201706.0127

- 1382 .v1
- 1383 Breton, S., Stewart, D. T., Shepardson, S., Trdan, R. J., Bogan, A. E., Chapman,
1384 E. G., ... Hoeh, W. R. (2010). Novel protein genes in animal mtDNA: A
1385 new sex determination system in freshwater mussels (bivalvia: Unionoida)?
1386 *Molecular Biology and Evolution*, 28(5), 1645–1659. doi: 10.1093/molbev/
1387 msq345
- 1388 Budd, A., Banh, Q., Domingos, J., & Jerry, D. (2015). Sex control in fish: Ap-
1389 proaches, challenges and opportunities for aquaculture. *Journal of Marine
1390 Science and Engineering*, 3(2), 329–355. doi: 10.3390/jmse3020329
- 1391 Burdon, D., Callaway, R., Elliott, M., Smith, T., & Wither, A. (2014, 04).
1392 Mass mortalities in bivalve populations: A review of the edible cockle
1393 *Cerastoderma edule* (l.). *Estuarine, Coastal and Shelf Science*, 150. doi:
1394 10.1016/j.ecss.2014.04.011
- 1395 Campos, A., Tedesco, S., Vasconcelos, V., & Cristobal, S. (2012). Proteomic
1396 research in bivalves: Towards the identification of molecular markers of
1397 aquatic pollution. *Proteomic Research in Bivalves*, 75(14), 4346–4359. doi:
1398 10.1016/j.jprot.2012.04.027
- 1399 Cerqueira, V., Santos, M., Baghoussi, Y., & Soares, C. (2024). On-the-fly data
1400 augmentation for forecasting with deep learning. *ArXiv (Cornell Univer-
1401 sity)*. Retrieved from <https://doi.org/10.48550/arxiv.2404.16918>
- 1402 Coe, W. R. (1943). Sexual differentiation in mollusks. i. pelecypods. *The Quarterly
1403 Review of Biology*, 18, 154–164. doi: 10.1086/qrb.1943.18.issue-2
- 1404 Collin, R. (2013). Phylogenetic patterns and phenotypic plasticity of molluscan
1405 sexual systems. *Integrative and Comparative Biology*, 53, 723–735. doi:
1406 10.1093/icb/ict076
- 1407 Concepcion, R., Guillermo, M., Tanner, S. E., Fonseca, V., & Duarte, B. (2023).
1408 Bivalvenet: A hybrid deep neural network for common cockle (*cerastoderma
1409 edule*) geographical traceability based on shell image analysis. *Ecological
1410 Informatics*, 78, 102344. doi: 10.1016/j.ecoinf.2023.102344
- 1411 Cui, Y., Pan, T., Chen, S., & Zou, X. (2020). A gender classification method
1412 for chinese mitten crab using deep convolutional neural network. *Multi-
1413 media Tools and Applications*, 79(11-12), 7669–7684. doi: <https://doi.org/10.1007/s11042-019-08355-w>
- 1415 Davenport, J., & Wong, T. (1986, September). Responses of the blood cockle
1416 *Anadara granosa* (l.) (bivalvia: Arcidae) to salinity, hypoxia and aerial ex-
1417 posure. *Aquaculture*, 56(2), 151–162. Retrieved from [https://doi.org/10.1016/0044-8486\(86\)90024-4](https://doi.org/10.1016/0044-8486(86)90024-4) doi: 10.1016/0044-8486(86)90024-4
- 1419 Doering, P., & Ludwig, J. (1990). Shape analysis of otoliths—a tool for indirect
1420 ageing of eel, *anguilla anguilla* (l.)? *International Review of Hydrobiology*,
1421 75(6), 737–743. doi: 10.1002/iroh.19900750607
- 1422 Erica, D. (2018, April 4). *Clam dissection: A first step into dissection and
1423 anatomy for young learners*. Rosie Research. Retrieved from <https://>

- 1424 rosiereresearch.com/clam-dissection-anatomy/
- 1425 Fao 2024 report: Sustainable aquatic food systems important for global food
1426 security – european fishmeal. (2024). <https://effop.org/news-events/fao-2024-report-sustainable-aquatic-food-systems-important-for-global-food-security/>.
- 1429 Ferguson, G. J., Ward, T. M., & Gillanders, B. M. (2011). Otolith shape and
1430 elemental composition: Complementary tools for stock discrimination of
1431 mulloway (*argyrosomus japonicus*) in southern australia. *Fish Research*,
1432 110, 75–83. doi: 10.1016/j.fishres.2011.03.014
- 1433 GeeksforGeeks. (2020, August 6). *Stratified k fold cross validation*. Retrieved from <https://www.geeksforgeeks.org/stratified-k-fold-cross-validation/>
- 1436 GeeksforGeeks. (2024, May). *Cross-validation using k-fold with scikit-learn*. Retrieved from <https://www.geeksforgeeks.org/cross-validation-using-k-fold-with-scikit-learn/> (Accessed: 2025-04-23)
- 1439 Gosling, E. (2004). *Bivalve molluscs: biology, ecology and culture*. Oxford: Blackwell Science.
- 1441 Heller, J. (1993). Hermaphroditism in molluscs. *Biological Journal of the Linnean Society*, 48, 19–42. doi: 10.1111/bij.1993.48.issue-1
- 1443 Hussain, S. S., & Zaidi, S. S. H. (2024). Adaboost ensemble approach with
1444 weak classifiers for gear fault diagnosis and prognosis in dc motors. *Applied Sciences*, 14(7), 3105. doi: 10.3390/app14073105
- 1446 Ishak, A. R., Mohamad, S., Soo, T. K., & Hamid, F. S. (2016). Leachate and
1447 surface water characterization and heavy metal health risk on cockles in
1448 kuala selangor. In *Procedia - social and behavioral sciences* (Vol. 222, pp.
1449 263–271). doi: 10.1016/j.sbspro.2016.05.156
- 1450 Jaiswal, S. (2024, January 4). *What is normalization in machine learning? a comprehensive guide to data rescaling*. DataCamp. Retrieved from <https://www.datacamp.com/tutorial/normalization-in-machine-learning> (Accessed 2025-04-23)
- 1454 Karapunar, B., Werner, W., Fürsich, F. T., & Nützel, A. (2021). The earliest
1455 example of sexual dimorphism in bivalves—evidence from the astartid
1456 *Nicanella* (lower jurassic, southern germany). *Journal of Paleontology*,
1457 95(6), 1216–1225. doi: 10.1017/jpa.2021.48
- 1458 Kerr, L. A., & Campana, S. E. (2014). Chemical composition of fish hard parts
1459 as a natural marker of fish stocks. In *Stock identification methods* (pp. 205–
1460 234). Elsevier. doi: 10.1016/b978-0-12-397003-9.00011-4
- 1461 Kim, E., Yang, S.-M., Cha, J.-E., Jung, D.-H., & Kim, H.-Y. (2024). Deep
1462 learning-based phenotype classification of three ark shells: Anadara kagoshimensis,
1463 tegillarca granosa, and anadara broughtonii. *Frontiers in Marine Science*, 11. doi: 10.3389/fmars.2024.1356356
- 1465 Lee, J. H. (1997). Studies on the gonadal development and gametogenesis of the

- 1466 granulated ark, tegillarca granosa (linne). *The Korean Journal of Malacology*, 13, 55–64.
- 1467
- 1468 Leguá, J., Plaza, G., Pérez, D., & Arkhipkin, A. (2013). Otolith shape analysis as
1469 a tool for stock identification of the southern blue whiting, micromesistius
1470 australis. *Latin American Journal of Aquatic Research*, 41, 479–489.
- 1471 Mahé, K., Oudard, C., Mille, T., Keating, J., Gonçalves, P., Clausen, L. W., &
1472 et al. (2016). Identifying blue whiting (micromesistius poutassou) stock
1473 structure in the northeast atlantic by otolith shape analysis. *Canadian
1474 Journal of Fisheries and Aquatic Sciences*, 73, 1363–1371. doi: 10.1139/
1475 cjfas-2015-0332
- 1476 May, K., Maung, C., Phy, E., & Tun, N. (2021). Spawning period of blood cockle
1477 tegillarca granosa (linnaeus, 1758) in myeik coastal areas. *J. Myanmar Acad.
1478 Arts Sci*, 4.
- 1479 Miranda, D. V., & Ferriols, V. M. E. N. (2023). Initial attempts on spawning and
1480 larval rearing of the blood cockle, tegillarca granosa (linnaeus, 1758), in the
1481 philippines. *Asian Fisheries Science*, 36(2). doi: 10.33997/j.afs.2023.36.2
1482 .001
- 1483 Mérigot, B., Letourneur, Y., & Lecomte-Finiger, R. (2007). Characterization of
1484 local populations of the common sole solea solea (pisces, soleidae) in the nw
1485 mediterranean through otolith morphometrics and shape analysis. *Marine
1486 Biology*, 151(3), 997–1008. doi: 10.1007/s00227-006-0549-0
- 1487 Nahm, F. S. (2022). Receiver operating characteristic curve: Overview and
1488 practical use for clinicians. *Korean Journal of Anesthesiology*, 75(1), 25–
1489 36. Retrieved from <https://doi.org/10.4097/kja.21209> doi: 10.4097/
1490 kja.21209
- 1491 Narasimham, K. A. (1988). Taxonomy of the blood clams anadara (tegillarca)
1492 granosa (linnaeus, 1758) and a. (t.) rhombea (born, 1780).
- 1493 Naylor, R. L., Goldburg, R. J., Primavera, J. H., Kautsky, N., Beveridge,
1494 M. C. M., Clay, J., ... Troell, M. (2000). Effect of aquaculture on world
1495 fish supplies. *Nature*, 405(6790), 1017–1024. doi: 10.1038/35016500
- 1496 Ponton, D. (2006). Is geometric morphometrics efficient for comparing otolith
1497 shape of different fish species? *Journal of Morphology*, 267(7), 750–757.
1498 doi: 10.1002/jmor.10439
- 1499 Quenu, M., Trewick, S. A., Brescia, F., & Morgan-Richards, M. (2020). Geometric
1500 morphometrics and machine learning challenge currently accepted species
1501 limits of the land snail placostylus (pulmonata: Bothriembryontidae) on the
1502 isle of pines, new caledonia. *Journal of Molluscan Studies*, 86(1), 35–41.
1503 doi: 10.1093/mollus/eyz031
- 1504 Ribeiro, D. (2024, Aug.). *Diogo ribeiro. data science. kruskal-wallis test.*
1505 Retrieved from https://diogoribeiro7.github.io/statistics/data%20analysis/kruskal_wallis/ (Accessed: 2025-04-23)
- 1506
- 1507 Sany, S. B. T., Hashim, R., Rezayi, M., Salleh, A., Rahman, M. A., Safari, O.,

- 1508 & Sasekumar, A. (2014). Human health risk of polycyclic aromatic hydro-
1509 carbons from consumption of blood cockle and exposure to contaminated
1510 sediments and water along the klang strait, malaysia. *Marine Pollution*
1511 *Bulletin*, 84(1-2), 268–279. doi: 10.1016/j.marpolbul.2014.05.004
- 1512 Srisunont, C., Nobpakhun, Y., Yamalee, C., & Srisunont, T. (2020). Influence
1513 of seasonal variation and anthropogenic stress on blood cockle (*Tegillarca*
1514 *granosa*) production potential. *Influence of Seasonal Variation and Anthro-*
1515 *pogenic Stress on Blood Cockle (*Tegillarca Granosa*) Production Potential*,
1516 44(2), 62–82.
- 1517 Tarca, A. L., Carey, V. J., Chen, X.-w., Romero, R., & Drăghici, S. (2007). Ma-
1518 chine learning and its applications to biology. *PLoS Computational Biology*,
1519 3(6), e116. doi: 10.1371/journal.pcbi.0030116
- 1520 Team, K. (n.d.). *Keras documentation: Reducelronplateau*. Retrieved from
1521 https://keras.io/api/callbacks/reduce_lr_on_plateau/
- 1522 Thompson, R. J., Newell, R. I. E., Kennedy, V. S., & Mann, R. (1996). Repro-
1523 ductive process and early development. In V. S. Kennedy, R. I. E. Newell,
1524 & A. F. Eble (Eds.), *The eastern oyster crassostrea virginica* (pp. 335–370).
1525 College Park, MD: Maryland Sea Grant.
- 1526 Tsutsumi, M., Saito, N., Koyabu, D., & Furusawa, C. (2023). A deep learning
1527 approach for morphological feature extraction based on variational auto-
1528 encoder: An application to mandible shape. *Npj Systems Biology and Ap-*
1529 *plications*, 9(1), 1–12. doi: 10.1038/s41540-023-00293-6
- 1530 Wong, T. M., & Lim, T. G. (2018). *Cockle (anadara granosa) seed produced in*
1531 *the laboratory, malaysia*. (Handle.net) doi: 10.3366/in_3366.pdf
- 1532 Zahn, C. T., & Roskies, R. Z. (1972). Fourier descriptors for plane closed curves.
1533 *IEEE Transactions on Computers*, C-21, 269–281. doi: 10.1109/tc.1972
1534 .5008949
- 1535 Zelditch, M., Swiderski, D. L., & Sheets, H. D. (2004). *Geometric morphometrics*
1536 *for biologists: A primer* (2nd ed.). Waltham: Elsevier Academic Press.
- 1537 Zha, S., Tang, Y., Shi, W., Liu, H., Sun, C., Bao, Y., & Liu, G. (2022). Im-
1538 pacts of four commonly used nanoparticles on the metabolism of a ma-
1539 rine bivalve species, *Tegillarca granosa*. *Chemosphere*, 296, 134079. doi:
1540 10.1016/j.chemosphere.2022.134079
- 1541 Zhan, P. L., Zha, S., & Bao, Y. (2022). Hypoxia-mediated immunotoxicity in the
1542 blood clam *Tegillarca granosa*. *Marine Environmental Research*, 177. Re-
1543 trieved from <https://doi.org/10.1016/j.marenvres.2022.105632>

₁₅₄₄ **Appendix A**

₁₅₄₅ **Data Gathering Documentation**



Figure A.1: Sex Identification Through Spawning of *Tegillarca granosa*



Figure A.2: Sex-Based Separation of *Tegillarca granosa* Samples Post-Spawning



Figure A.3: Sex Identified Female Through Dissection of *Tegillarca granosa*



Figure A.4: Sex Identified Male Through Dissection of *Tegillarca granosa*

Litob_Id	Length	Width	Height	Rib count	Length (Hinge Line)	Distance Umbos
10001	48.05	37.6	32.15	20	33.55	4.1
20001	48.05	37.6	32.15	20	33.55	4.1
30001	48.05	37.6	32.15	20	33.55	4.1
40001	48.05	37.6	32.15	20	33.55	4.1
50001	48.05	37.6	32.15	20	33.55	4.1
60001	48.05	37.6	32.15	20	33.55	4.1
10002	47.4	32.5	32.25	20	33.1	3.05
20002	47.4	32.5	32.25	20	33.1	3.05
30002	47.4	32.5	32.25	20	33.1	3.05
40002	47.4	32.5	32.25	20	33.1	3.05
50002	47.4	32.5	32.25	20	33.1	3.05
60002	47.4	32.5	32.25	20	33.1	3.05
10003	43.3	34.1	31.25	21	32.05	4.5
20003	43.3	34.1	31.25	21	32.05	4.5
30003	43.3	34.1	31.25	21	32.05	4.5
40003	43.3	34.1	31.25	21	32.05	4.5
50003	43.3	34.1	31.25	21	32.05	4.5
60003	43.3	34.1	31.25	21	32.05	4.5
10075	50.05	35.05	32.05	21	30.05	4.1
20075	50.05	35.05	32.05	21	30.05	4.1

Figure A.5: Linear Measurements of Female *Tegillarca granosa*

Litob_Id	Length	Width	Height	Rib count	Length (Hinge Line)	Distance Umbos
110004	43.1	33.05	28.15	21	28.5	3.05
120004	43.1	33.05	28.15	21	28.5	3.05
130004	43.1	33.05	28.15	21	28.5	3.05
140004	43.1	33.05	28.15	21	28.5	3.05
150004	43.1	33.05	28.15	21	28.5	3.05
160004	43.1	33.05	28.15	21	28.5	3.05
110005	41.1	31.05	27.6	20	23.05	3.35
120005	41.1	31.05	27.6	20	23.05	3.35
130005	41.1	31.05	27.6	20	23.05	3.35
140005	41.1	31.05	27.6	20	23.05	3.35
150005	41.1	31.05	27.6	20	23.05	3.35
160005	41.1	31.05	27.6	20	23.05	3.35
110006	43.2	33.45	29.35	20	29.35	3.3
120006	43.2	33.45	29.35	20	29.35	3.3
130006	43.2	33.45	29.35	20	29.35	3.3
140006	43.2	33.45	29.35	20	29.35	3.3
150006	43.2	33.45	29.35	20	29.35	3.3
160006	43.2	33.45	29.35	20	29.35	3.3
110007	41.5	32.55	27.7	20	24.1	3.7
120007	41.5	32.55	27.7	20	24.1	3.7

Figure A.6: Linear Measurements of Male *Tegillarca granosa*

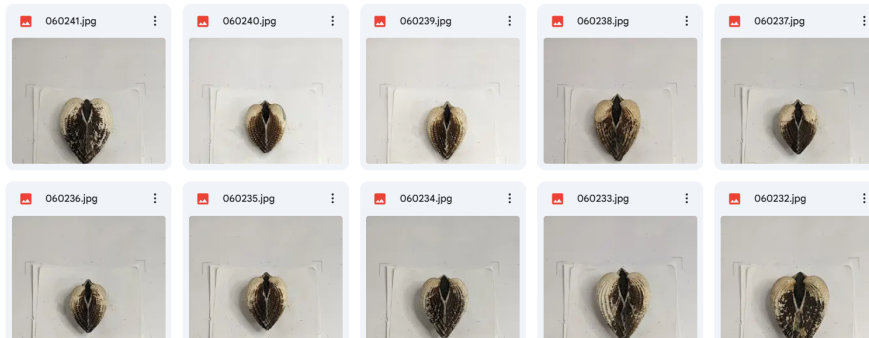


Figure A.7: Captured Images of Female *Tegillarca granosa*

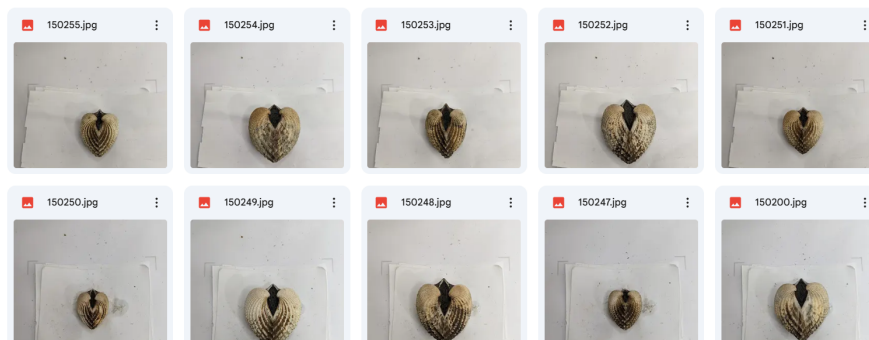


Figure A.8: Captured Images of Male *Tegillarca granosa*

1546 **Appendix B**

1547 **Supplementary Analysis**

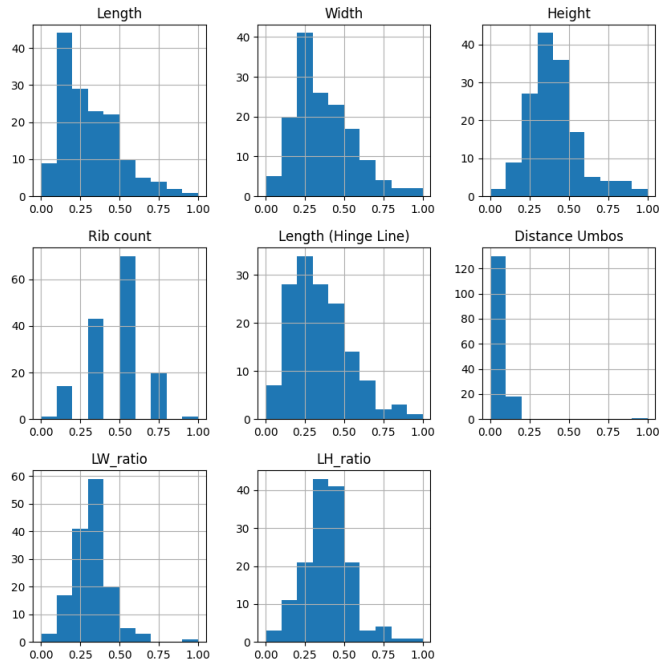


Figure B.1: Feature Distribution of *Tegillarca granosa*

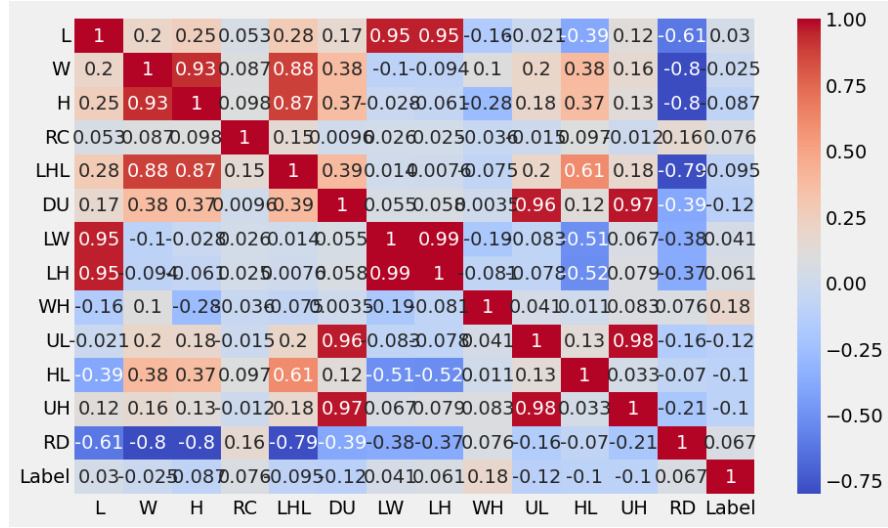


Figure B.2: Correlation Matrix of Morphological Variables *Tegillarca granosa*

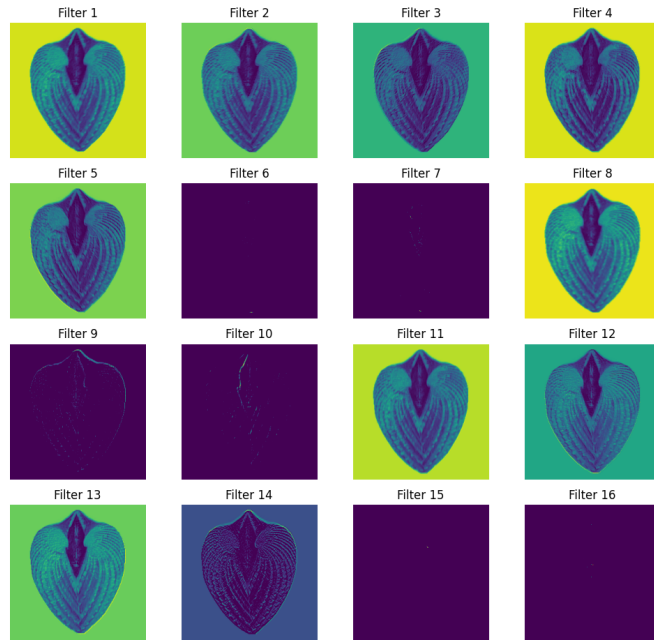


Figure B.3: Feature Maps from First Convolution Layer

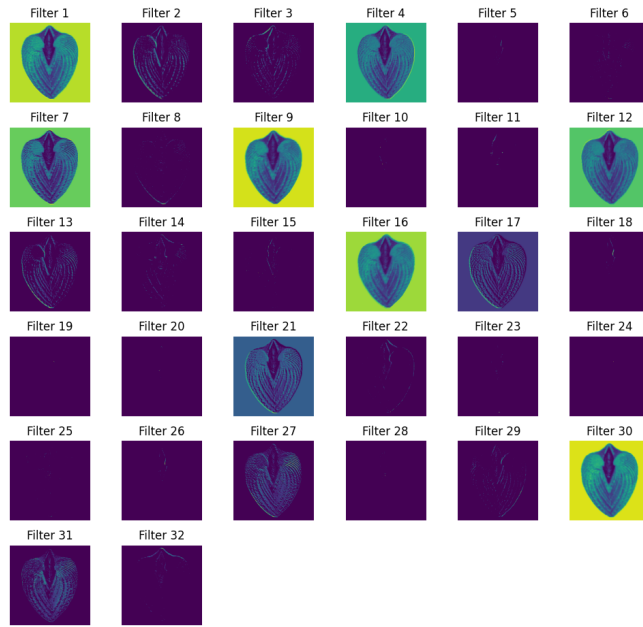


Figure B.4: Feature Maps from Second Convolution Layer

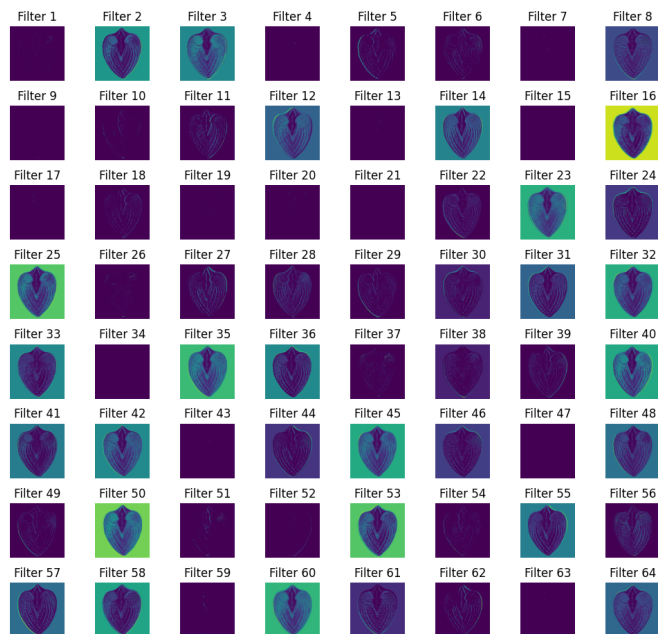


Figure B.5: Feature Maps from Third Convolution Layer